1. Report No. FHWA/LA.00/355	2. Government Accession No.	3. Recipient's Catalog No.
4. Title and Subtitle Effect of Moisture Content and Dry Unit Weight on the Resilient Modulus of Subgrade Soils Predicted by Cone Penetration Test	5. Report Date June 2002	
	6. Performing Organization Code 98-8GT	
7. Author(s) Louay N. Mohammad, Ph.D., Hani H. Titi, Ph.D., P.E., Ananda Herath, Ph.D., P.E.	8. Performing Organization Report No. 355	
9. Performing Organization Name and Address Louisiana Transportation Research Center Louisiana State University Baton Rouge, LA 70803	10. Work Unit No.	
	11. Contract or Grant No. 98-8GT	
12. Sponsoring Agency Name and Address FHWA Office of Technology Application 400 7th Street, SW Washington, DC 20590 DOTD P. O. Box 94245 Baton Rouge, LA 70804	13. Type of Report and Period Covered Final Report 5/2000 - 6/2002	
	14. Sponsoring Agency Code	

15. Supplementary Notes
Conducted in Cooperation with the United States Department of Transportation, Federal Highway Administration

16. Abstract
The objective of this study was to investigate the effect of moisture content and dry unit weight on the resilient characteristics of subgrade soil predicted by the cone penetration test. An experimental program was conducted in which cone penetration tests, repeated load triaxial tests, and soil property tests were performed. An experimental setup was fabricated to conduct laboratory cone penetration tests on compacted soil samples. Four soil types and three levels of moisture contents - dry side, optimum, and wet side - were selected for these testings. The results of the laboratory tests were used to validate the prediction models developed during phase I of this research. The application of the cone penetration test in evaluating subgrade soil resilient modulus was successful.

17. Key Words Resilient Modulus, Miniature Cone Penetrometer, Subgrade Soils		18. Distribution Statement Unrestricted. This document is available through the National Technical Information Service, Springfield, VA 21161.	
19. Security Classif. (of this report)	20. Security Classif. (of this page)	21. No. of Pages 86	22. Price

Effect of Moisture Content and Dry Unit Weight on the Resilient Modulus of Subgrade Soils Predicted by Cone Penetration Test

by

Louay N. Mohammad, Ph.D.
Associate Professor of Civil and Environmental Engineering
Director, Engineering Materials Characterization Research Facility
Louisiana Transportation Research Center
Louisiana State University

Hani H. Titi, Ph.D., P.E.
Assistant Professor
Department of Civil Engineering and Mechanics
College of Engineering and Applied Science
University of Wisconsin, Milwaukee

Ananda Herath, Ph.D., P.E.
Postdoctoral Researcher,
Louisiana Transportation Research Center

FHWA Contract No. DTFH71-97-PTP-LA -14
LTRC Project No. 98-8GT
State Project No. 736-99-0582

conducted for

Louisiana Department of Transportation and Development
Louisiana Transportation Research Center

June 2002

ABSTRACT

The objective of this study was to investigate the effect of moisture content and dry unit weight on the resilient characteristics of subgrade soil predicted by the cone penetration test. An experimental program was conducted in which cone penetration tests, repeated load triaxial tests, and soil property tests were performed. An experimental setup was fabricated to conduct laboratory cone penetration tests on compacted soil samples. Four soil types and three levels of moisture contents - dry side, optimum, and wet side - were selected for these testings. The results of the laboratory tests were used to validate the prediction models developed during phase I of this research. The application of the cone penetration test in evaluating subgrade soil resilient modulus was successful.

ACKNOWLEDGMENTS

This research project is financially supported by the U.S. Department of Transportation, Federal Highway Administration/Priority Technology Program (USDOT FHWA/PTP), the Louisiana Department of Transportation and Development (DOTD), and the Louisiana Transportation Research Center (LTRC).

The effort of William T. Tierney, Research Specialist/LTRC, in conducting the cone penetration tests and soil sampling is appreciated. The assistance of Amar Raghavendra, Research Associate/ LTRC, in getting the MTS system operational for the resilient modulus tests is acknowledged. The effort and cooperation of Mark Morvant, Geotechnical and Pavement Administrator/LTRC, during the field and laboratory testing programs is gratefully appreciated. Paul Brady, Melba Bounds, and Kenneth Johnson, LTRC Geotechnical Laboratory, helped in conducting various soil tests.

IMPLEMENTATION IN PAVEMENT DESIGN

The proposed procedure is to be implemented in designs, rehabilitation, and quality control and quality assurance of pavements. A software program is to be developed to implement the proposed models in these pavement applications.

TABLE OF CONTENTS

LIST OF TABLES

LIST OF FIGURES

INTRODUCTION

The American Association of State Highway and Transportation Officials (AASHTO) guide for design of pavement structures recommends the use of the resilient modulus for characterization of base and subgrade soil and for design of flexible pavements *[1]*. The subgrade soil characterization, based on the resilient modulus, is a realistic way to analyze the moving vehicle loads on a pavement. The resilient modulus represents the dynamic stiffness of pavement materials under the repeated loads of vehicles.

A major research effort was undertaken at the Louisiana Transportation Research Center (LTRC) to investigate the applicability of the intrusion technology to estimate the resilient modulus of subgrade soils. The research also intended to develop a methodology to predict the resilient modulus from the cone penetration test (CPT) parameters. The research was performed in two phases: phase I and phase II.

Phase I of this study, "Investigation of the Applicability of Intrusion Technology to Estimate the Resilient Modulus of Subgrade Soil," was completed in the year 2000 *[19]*. This report presents the results of phase II of a major research effort conducted to investigate the applicability of the intrusion technology in estimating the resilient modulus of subgrade soils. Phase II of this study investigated the effect of moisture content and dry unit weight on the predicted resilient modulus by the cone penetration test. A brief description of the phase I is given below.

In phase I, the results of the research demonstrated the applicability of the intrusion technology to predict the resilient modulus of subgrade soils. Common Louisiana subgrade soil types were subjected to field and laboratory testing programs. Field tests consisted of cone penetration tests using two cone penetrometers, the 15 cm^2 and the 2 cm^2. Undisturbed and disturbed soil samples were collected from the test sites for the laboratory-testing program. Laboratory tests consisted of tests to determine the physical and strength characteristics of the soils. Repeated load triaxial tests were conducted on the undisturbed soil samples to determine the resilient modulus according to the AASHTO T 294 *[2]*. Statistical analysis was conducted in which correlations among the resilient modulus, soil physical properties, and cone parameters were proposed. These correlations were verified and validated based on the field tests. The successful accomplishment of phase I demonstrated the need to further investigate the effect of the soil properties on the resilient modulus of soils.

Phase I: Development of Resilient Modulus Models

The details of the model development are given in the field testing program *[19]*.

A Model for Fine-grained Soils (In-situ Stresses)

The following model was developed for fine-grained soil with consideration of in-situ stresses.

$$\frac{M_r}{s_c^{0.55}} = \frac{1}{s_v}\left(31.79 q_c + 74.81 \frac{f_s}{w}\right) + 4.08 \frac{g_d}{g_w} \quad (1)$$

where,

M_r- resilient modulus (MPa),

s_c- confining (minor principal) stress (kPa),

s_v- vertical (major principal) stress (kPa),

q_c- tip resistance(MPa),

f_s- sleeve friction (MPa),

w- water content (as a decimal),

g_d- dry unit weight (kN/m^3), and

g_w- unit weight of water (kN/m^3).

A Model for Coarse-grained Soils (In-situ Stresses)

The following model was developed for coarse-grained soil based on the in-situ stresses.

$$\frac{M_r}{s_c^{0.55}} = 6.66 \frac{(q_c s_b)}{s_v^2} - 32.99 \frac{f_s}{q_c} + 0.52 \frac{g_d}{(w g_w)} \quad (2)$$

where,

M_r- resilient modulus (MPa),

s_c- confining (minor principal) stress (kPa),

s_v- vertical (major principal) stress (kPa),

q_c- tip resistance(MPa),

f_s- sleeve friction (MPa),

w- water content (as a decimal),

g_d- dry unit weight (kN/m^3),

g_w- unit weight of water (kN/m^3), and

s_b - bulk stress.

A Model for Fine-grained Soil (Traffic and In-situ Stresses)

The following model was developed for fine-grained soil with consideration of traffic and in-situ stresses.

$$\frac{M_r}{s_3^{0.55}} = 47.03\frac{q_c}{s_1} + 170.40\frac{f_s}{s_1 w} + 1.67\frac{g_d}{g_w} \quad (3)$$

where,

M_r- resilient modulus (MPa),

s_3- minor principal stress (s_c- confining) (kPa),

s_1- major principal stress (s_v- vertical stress) (kPa),

q_c - tip resistance(MPa),

f_s- sleeve friction (MPa),

w- water content (as a decimal),

g_d- dry unit weight (kN/m^3), and

g_w- unit weight of water (kN/m^3).

A Model for Coarse-grained Soil (Traffic and In-situ Stresses)

The following model was developed for coarse-grained soil with consideration of traffic and in-situ stresses.

$$\frac{M_r}{s_3^{0.55}} = 18.95\frac{q_c s_b}{s_1^2} + 0.41\frac{g_d}{g_w w} \quad (4)$$

where,

M_r- resilient modulus (MPa),

s_3- confining (minor principal) stress (kPa),

s_1- major principal stress (kPa),

q_c - tip resistance(MPa),

w- water content (as a decimal),

g_d- dry unit weight (kN/m^3),

g_w- unit weight of water (kN/m^3), and

s_b - bulk stress.

Phase II :Controlled Laboratory Testing

Currently, the Louisiana Department of Transportation and Development (LA DOTD) procedure for estimating the resilient modulus of subgrade soils is based on the soil support value (SSV). However, soil support value does not represent the dynamic behavior under moving vehicles on pavements. The resilient modulus represents the dynamic behavior of pavements under the moving vehicles.

The resilient modulus is usually determined from laboratory or field nondestructive test methods (NDT). The laboratory procedures are considered laborious, time consuming, and highly expensive. The field nondestructive test procedures have certain limitations with respect to repeatability of test results. The shortcomings of these test methods signify the need for an in-situ technology for determining the resilient characteristics of subgrade and base soils underneath a pavement. The cone penetration testing is considered the most frequently used tool for characterization of geomedia. This is because the CPT is economical, fast, and provides repeatable and reliable results. The CPT is conducted by advancing a cylindrical rod with a cone tip into the soil and measuring the tip resistance and sleeve friction due to this intrusion. The cone resistance parameters, tip resistance, and sleeve friction are used to classify soil strata and to estimate strength and deformation characteristics of soils.

The American Association of State Highway and Transportation Officials (AASHTO) guide for design of pavement structures stipulates that determination of the resilient modulus of subgrade soils during different seasons of the year be necessary to account for the variations of the moisture content *[1]*. The year is usually divided into different time intervals during which the seasonal resilient modulus values are determined. The minimum time interval shall not be less than one-half month for any season. In this procedure, the seasonal resilient modulus values are assigned in their corresponding time periods. Then the seasonal resilient modulus values are converted to the effective design resilient modulus values. For rigid pavements, the resilient modulus of subgrade is used to determine the effective modulus of subgrade reaction (k-value). In the field, subgrade soils encounter wetting and drying cycles. The subgrade resilient modulus increases as soil dries out. The resilient modulus is expected to decrease in a wet period. Therefore, the laboratory resilient modulus test should be performed in wet seasons and dry seasons since they change the subgrade soil resilient modulus. Both the resilient modulus and cone penetration test parameters are affected by the moisture content and unit weight of soils.

A laboratory cone penetration testing program was performed to study the effect of moisture content and unit weight on the resilient modulus and cone penetration test parameters. The laboratory cone penetration tests were performed on four soil types (silty clay, heavy clay, silt, and sand) with three different moisture-unit weight combinations (dry side, optimum, and wet side). This study presents twelve laboratory cone penetration tests on four soil types with different moisture-unit weight combinations. In addition to these tests, resilient modulus, soil classification, specific gravity, triaxial, Atterberg limit, moisture content, and unit weight tests were performed. The laboratory cone penetration and resilient modulus test results were interpreted by the correlations developed in phase I of this study. A sensitivity analysis was performed to study the effect of resilient modulus on overlay thickness in pavements. The current LA DOTD procedure for estimating the resilient modulus was compared with the proposed procedure in this study. A procedure for approximate estimation of dry unit weight of soils is presented. A procedure for use of the proposed models in predicting the seasonal variations in resilient modulus is presented. A procedure for use of the proposed models in predicting the resilient modulus profile is suggested.

Background

Resilient Modulus

The resilient modulus is determined using the backcalculation of the nondestructive test deflection results, laboratory triaxial testing on soil samples, and correlations with soil properties, California Bearing Ratio (CBR), and soil support values. The Dynaflect, Road Rater, and Falling Weight Deflectometer (FWD) are the devices used for NDT test methods. These NDT methods measure the deflection of the pavement under a loading where deflections are used in backcalculation subroutines to estimate the resilient modulus. Backcalculated modulus depends on many factors, such as loading condition and stiffness in layers *[32], [10]*.

There are many laboratory testing devices used for determining the resilient modulus of subgrade soil. The devices used for laboratory testings are triaxial cell, resonant column, simple shear device, torsional apparatus, hollow cylinder and true triaxial cell. Because of its simplicity, repeatability and accuracy, the triaxial cell is the most popular laboratory testing device. But these laboratory tests are laborious, time consuming, and expensive.

In 1986, AASHTO recommended the testing procedure, T 274-82, to determine the resilient modulus of subgrade soil. Inadequate conditioning steps and over stressing the sample were

reported in this test procedure *[13], [23]*. The major drawback of the T 274-82 was that the stresses were so high that the specimen may be damaged in the preconditioning stage. The AASHTO T 274-82 test procedure was modified and replaced by an interim AASHTO procedure T 292-91I. Then in 1992, AASHTO adopted the Strategic Highway Research Program (SHRP) Protocol 46 (AASHTO T 294-92I). After including the previous developments in the test procedure for determination of the resilient modulus of subgrade soil, the current test procedure, T 294-94, was introduced *[2]*. This procedure requires a test system that includes a triaxial cell, a closed loop electro-hydraulic repeated loading system, load and specimen response control system, and measurement and recording system. Figure 1 shows the load pulse used in this test method. In order to simulate traffic loadings, AASHTO T 294-94 recommends the haversine-shaped load pulse with a 0.1 second load followed by a 0.9 second rest period.

Resilient modulus is influenced by many factors. Many investigators observed an increase in resilient modulus of granular materials with increase in confining pressure *[27]*, *[9]*, *[14]*, *[15]*. This is due to the fact that increase in stiffness and decrease in dilational properties of granular soil.

The resilient modulus of cohesive soil decreases as deviator stress increases *[7]*. The same observations were made by several researchers for cohesive soils *[18], [12], [17]*. These observations confirm the stress and dilational property dependent nature of the resilient modulus of subgrade soil. Many researchers have studied the effect of moisture content on resilient modulus of soil *[4], [20], [16], [6], [19]*. They reported that resilient modulus of cohesive soil decreases as the moisture content increases. The resilient modulus can be influenced by the seasonal variation of moisture in soil, such as repeated freeze-thaw cycle. Several investigators reported that the resilient modulus can also be influenced by dry unit weight, size of the specimen, stress pulse shape, duration, frequency and sequence of stress levels, testing equipment, and specimen preparation as well as conditioning methods *[21], [14], [15]*.

Several empirical correlations have been developed to predict the results of the resilient modulus test *[36], [1], [25], [3], [18], [19], [12], [17]*. For granular materials, the relationship given below may be used as recommended by the AASHTO.

$$M_r = k_1 q^{k_2} \tag{5}$$

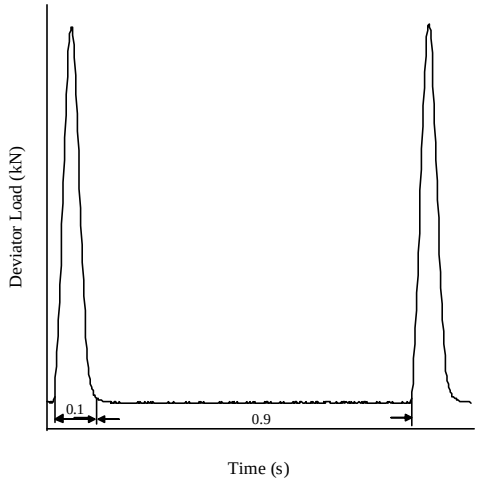

Figure 1
Load pulse used in the AASHTO T 294 testing procedure

This is known as the bulk stress model. The AASHTO recommended the deviator stress model for cohesive soil. It is given by,

$$M_r = k_3 s_d^{k_4} \tag{6}$$

where,

M_r - resilient modulus,

σ_d - deviator stress = s_1 - s_3, s_1- major principal stress,

s_2- intermediate principal stresses,

s_3 -minor principal stress,

θ - bulk stress = $s_1 + s_2 + s_3$, and

k_1 , k_2 , k_3,and k_4 - material constants.

The bulk stress model is very simple. However, the bulk stress model does not show individual effects of the deviator and confining stresses while the deviator stress model does not show the significance of the confining stress on cohesive soil *[35], [21]*.

Mohammad et al. proposed an octahedral stress model to over come some of the limitations discussed above *[12]*. This model takes into account the effects of shear and influence of the stress state. This model can be used for both fine-grained and coarse-grained soils. The model considers the octahedral shear and normal stresses. The octahedral model is given as follows,

$$\frac{M_r}{s_{atm}} = k_1 \left(\frac{s_{oct}}{s_{atm}} \right)^{k_2} \left(\frac{t_{oct}}{s_{atm}} \right)^{k_3} \quad (7)$$

where,

M_r -resilient modulus,

k_1 , k_2, and k_3 - material constants,

σ_{oct} -octahedral normal stress,

τ_{oct} -octahedral shear stress, and

σ_{atm} -atmospheric pressure (σ_{atm}= 101.35 kPa).

Many researchers correlated resilient modulus with strength and physical properties of soil such as California Bearing Ratio, moisture content, plasticity index, confining pressure and deviator stress *[1], [3], [5], [12], [17], [26], [19]*. But these models have to be calibrated and validated for local conditions.

Cone Penetration Test

The cone penetration test provides a rapid, continuous reading of tip resistance (q_c) and sleeve friction (f_s) as the cone penetrates into the ground. As shown in Figure 2, the CPT consists of a series of cylindrical push rods with a cone at the bottom. The penetration resistance is related to the strength of the soil. The tip resistance depends on the size of the cone tip, rate of penetration, types of soil, density and moisture content *[31]*. The standard cone has a projected tip area of 10 cm^2 and an apex angle of 60 degrees. A typical friction sleeve, located immediately above the tip, has 150 cm^2 surface area for the 10 cm^2 cones and 200 cm^2 for the 15 cm^2 cones. A 20 mm/sec penetration rate is normally used in the standard tests. The CPT and piezocone penetration tests (with pore water pressure measurements) (PCPT) have been used to determine soil properties such as soil classification, shear modulus, friction angle, in-situ stress state, constrained modulus, stress history or over consolidation ratio, sensitivity, undrained strength, hydraulic conductivity, coefficient of consolidation, unit weight, and cohesion intercept *[37], [30], [28]*.

The cone penetration test has gained the popularity among other in-situ tests in the geotechnical area. This is due to the fact that cone penetration test is simple, economical, rapid, and its results are repeatable and reliable. In this study, the miniature cone penetration test was used to evaluate the resilient modulus of subgrade soil.

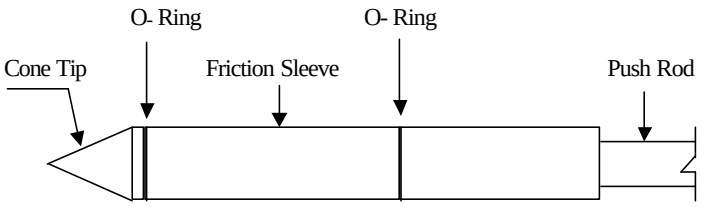

Figure 2
A typical friction cone penetrometer

Continuous Intrusion Miniature Cone Penetration Test (CIMCPT)

Tumay et al. developed the CIMCPT system, sponsored by the Priority Technology Program of the Federal Highway Administration, for site characterization of subgrade soil, construction control of embankments, assessment of the effectiveness of ground modification, and other shallow depth (upper 5 to 10 m) applications *[33]*, *[34]*. It is equipped with a miniature cone penetrometer test equipment. The miniature cone penetrometer used in this study has a cross sectional area of 2 cm^2 , friction sleeve area of 40 cm^2, and a cone apex angle of 60 degrees. The miniature cone is attached to a coiled push rod which replaces the segmental push rods in the standard cones. A 20 mm/sec penetration rate was used. The CIMCPT provides a finer soil profile as compared to the CPT. The miniature cone records a slightly higher tip resistance and lower sleeve friction than the 15 cm^2 cone does *[33]*, *[19]*.

OBJECTIVE

The objective of this study was to investigate the effect of the moisture content and unit weight of cohesive and cohesionless soils on the resilient modulus predicted by the miniature cone penetration test.

SCOPE

Laboratory controlled miniature cone penetration tests (using the 2 cm^2 miniature friction cone penetrometer) were conducted on four soils under three different moisture content-unit weight levels (dry, optimum, and wet side). The investigated soils were silty clay, heavy clay, sand, and silt. The resilient modulus of the investigated soils was conducted using the repeated load triaxial test.

METHODOLOGY

Laboratory testing program was conducted on four soils, which are silty clay, heavy clay, silt, and sand. The laboratory tests carried out consisted of miniature cone penetration testing and different soil tests to determine resilient modulus, physical properties, strength parameters, and compaction characteristics of the investigated soils.

Laboratory Cone Penetration Test Setup

An experimental setup was constructed at Louisiana Transportation Research Center (LTRC) to perform the laboratory cone penetration tests. As shown in Figure 3, the experimental setup consists of :

(1) a 55-gallon metal rigid wall container, 572 mm in diameter and 864 mm in height
(2) reaction frame of 1,130 mm in height and 1525 mm in width
(3) loading frame
(4) hydraulic loading system
(5) 2 cm^2 miniature cone penetrometer
(6) depth encoder system
(7) cone pushing and grabbing system
(8) control box
(9) computer and data acquisition system.

A special straight push rod with a length of 1,800 mm was made for this purpose and attached to the 2 cm^2 miniature cone for continuous intrusion. The hydraulic pushing system, mounted on a metal frame above the soil sample, consists of dual piston, double acting hydraulic jacks on a collapsible frame. A single stroke of the pushing system is 640 mm. This stroke is enough to penetrate a soil sample, used in this study, continuously at a rate of 20 mm/sec. An electronic analog to digital converter depth decoding system is employed to measure the depth at 4 mm intervals.

The data acquisition and collection system consists of a Pentium II computer collecting data from the cone penetrometer through the *DGH* modules *[33]*. The *DGH* modules are connected to different channels in the cone penetration test system, such as depth encoder and the strain gauges of tip and sleeve. The first *DGH, D1622*, is a pulse counter which is connected

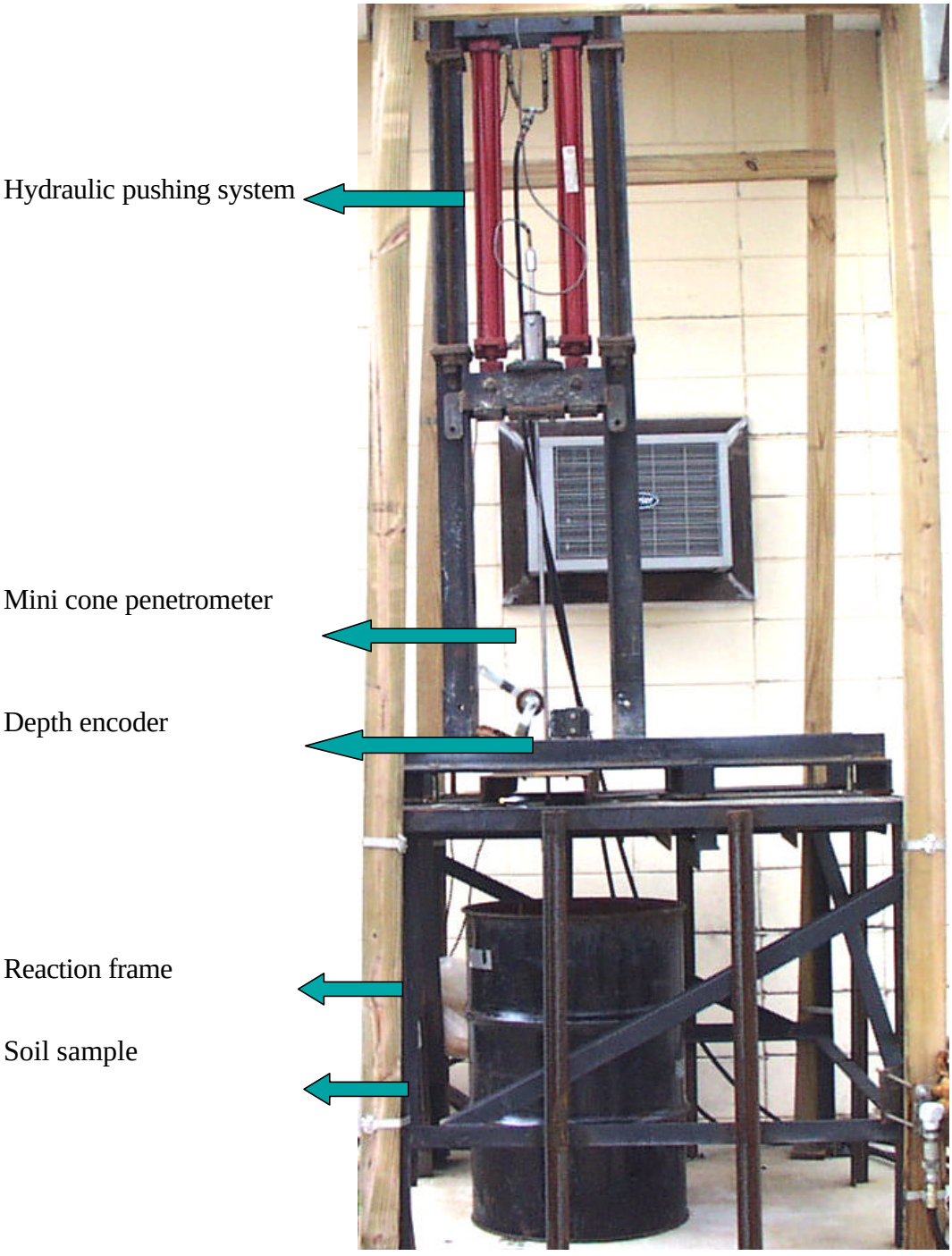

Figure 3
The laboratory cone test setup

to the depth encoder. The other two *DGH* modules are *D1102*, which measure voltage with a precision of ±10 mV. These two *DGH* modules are connected to the strain gauges of the tip and sleeve.

Resilient Modulus Testing Equipment

Repeated loading triaxial tests were conducted to determine the resilient modulus of the investigated soil using the MTS test system and following the AASHTO T 294 procedure. The heavy clay is very soft with a low unconfined compressive strength that could not be tested at high stress levels. In such cases, AASHTO T 294 specifies that the maximum deviator stress be limited to less than half of the unconfined compressive strength of the specimen. An MTS model 810 closed loop servo-hydraulic material testing system is used for applying repeated loading. The major components of this system are the loading system, digital controller, and load unit control panel. Details of this system are presented in phase I report of this research *[19]*.

Sample Preparation for Testing

Soil samples were prepared and compacted into the rigid wall chamber for cone penetration tests. Each soil type was subjected to the complete laboratory testing program under three different conditions of moisture content and unit weight. The standard Proctor test was performed to establish the moisture content-unit weight relationship for each soil. Then the three soil conditions (points) on the moisture-unit weight were identified. These points are the dry side point (about 3 to 5 percent less than the optimum moisture content), the optimum moisture content point, and wet side point (about 3 to 5 percent more than the optimum moisture content). The selected points in the moisture-unit weight curve are given in Table 1. The four soil types, heavy clay, silty clay, silt, and sand, were collected and dried in the oven. After oven dried, the soils were pulverized and passed through sieve No. 4 (4.75 mm). The weights of the dry soil (passing No. 4 sieve) and water, needed to bring the mixture unit weight to the target moisture content and unit weight, were determined. After establishing the number of layers to be compacted in the container, soil was mixed with the required amount of water in a mixing pan. After placing the required amount of wet soil for the first layer in the container, it was compacted until the required height was achieved. Fine-grained soils were compacted using an electric jack hammer, whereas coarse-grained soils were compacted

Table 1
Test points on the moisture-unit weight curve

Soil type		w (%)	γ_d (kN/m^3)
Silty clay	dry	14.4	16.1
	optimum	18.0	16.7
	wet	21.8	16.1
Heavy clay	dry	26.4	13.1
	optimum	31.4	13.6
	wet	36.4	12.8
Silt	dry	10.7	16.4
	optimum	15.2	17.2
	wet	20.4	15.9
Sand	dry	5.0	16.1
	optimum	8.1	16.4
	wet	11.0	15.7

using an electric vibrator. A certain selected pattern of compaction was followed. The compactor was moved on the soil surface very closely in a circular path starting from the center of the soil sample so that the entire soil surface path was compacted uniformly. Then the compactor was moved to the adjacent circular path and used to compact the soil similarly. This procedure continued until the compactor reached the rigid wall of the container. This path was reversed and this procedure was repeated until the required height was achieved. In this way, a uniform compaction effort was applied on the soil layer.

In order to determine the layer thickness, several compaction trials were performed with different layer depths. The results varied between 100 mm to 150 mm. After these compaction trials, each layer thickness in compaction was maintained at 125 mm. At least six layers were used for soil compaction. After compacting each layer, the top of the surface was scarified. This compaction procedure was repeated for the other layers.

Cone Penetration Tests

After compacting the soil in the container, the cone penetration test was performed using the miniature cone penetrometer. The test layout, as shown in Figure 4, was used in the laboratory cone test. Table 2 presents the summary of the testing program. Since the diameter of the

miniature cone penetrometer, used in this test, is 15.88 mm, this test layout allows to maintain a diameter ratio larger than 15. This test layout was selected to avoid the boundary effects. Cone penetration tests were performed continuously using the 2 cm^2 miniature cone penetrometer.

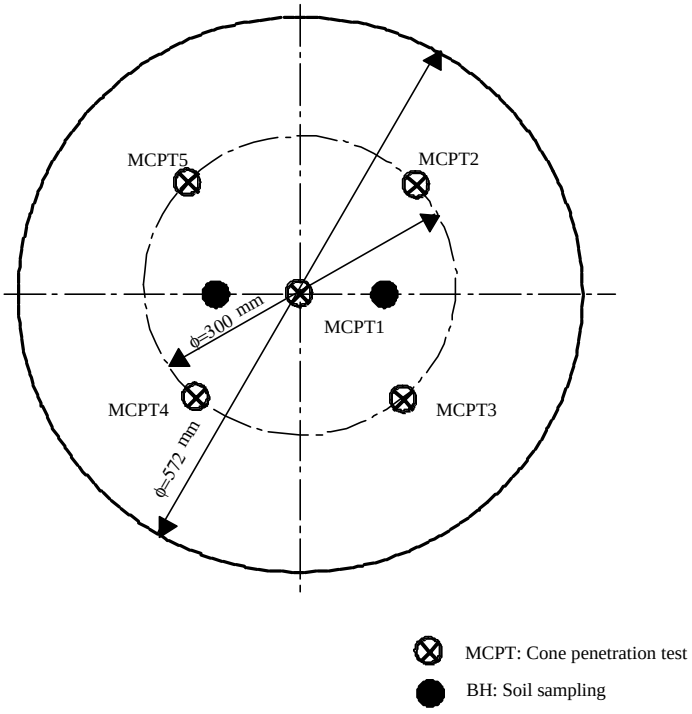

Figure 4
A typical layout for the laboratory cone test

Table 2
Laboratory cone testing program

Soil type	Tests	No. of tests
Silty clay	MCPT: Soil sampling:	5 2
Heavy clay	MCPT: Soil sampling:	5 2
Silt	MCPT: Soil sampling:	5 2
Sand	MCPT: Soil sampling:	5 2

Legend: MCPT- Miniature cone penetration test

Boundary Effects

The effects of the boundary of the container, used for soil sample testing, may influence on the test results. Cone penetration into a soil mass displaces a volume of soil equal to its own volume and causes a disturbances to the surrounding soil. This results in a ground heave in shallow penetration while primarily radial soil movement in deep penetration. But boundary effects can be minimized by selecting the cone testing locations away from the container's wall. Effect of the boundary condition on cone testing results depends on the diameter ratio, the soil sample diameter to cone diameter. Several studies discussed the boundary effects on the cone penetration test results *[8], [31], [24]*. Generally, the boundary of the container has no effect on the cone test results for the container diameter to cone diameter ratio larger than 15. According to Figure 4, the ratio maintained in this study was 36 at the center and 17 at the other four locations. This indicates a satisfactory clear distance was maintained in this study to avoid the boundary effects. The laboratory testing layout, shown in Figure 4, allows to perform cone penetration at different locations. This allows the uniformity of the sample as well as repeatability of the cone penetration test results to be checked.

Soil Testing Program

After conducting the cone penetration test, soil samples were collected at different depths from the container for the laboratory resilient modulus and soil property tests. Standard laboratory tests conducted on the soil samples were particle size analysis, Atterberg limits, specific

gravity, moisture content, standard compaction test, unconfined compression test, and consolidated undrained conventional triaxial compression (CU-CTC) test. The field density tests, sand cone test, and moisture test were performed at different depths to obtain the profile of unit weight and moisture content of tested soil.

Resilient modulus tests were performed on compacted soil samples from the investigated soils according to the AASHTO T 294. The soil samples were conditioned by applying one thousand repetitions of a specified deviator stress at a certain confining pressure. Conditioning eliminates the effects of specimen disturbances from sampling, compaction, and specimen preparation procedures and minimizes the imperfect contacts between end platens and the specimen. The specimen is then subjected to different stress sequences. The stress sequence is selected to cover the expected in-service range that a pavement or subgrade material experiences because of traffic loading.

ANALYSIS OF RESULTS

This section presents the results of the laboratory testing programs, analysis of these results, and critical evaluation of the test results. First, the analysis of the cone penetration test results is presented followed by the results and analysis of the repeated triaxial loading to evaluate the resilient modulus of the investigated soils. Finally, evaluation of the models proposed in the phase I and discussion of the results are presented.

Laboratory Cone Penetration Tests

In this section, effects of compaction, uniformity of the sample, and moisture-unit weight on the laboratory cone test results are discussed.

Table 3 presents the properties of silt and sand. The properties of silty clay and heavy clay were published in the report of phase I of this study *[19]*. The moisture-unit weight curves for silty clay, heavy clay, silt, and sand are shown in Figures 5, 6, 7, and 8, respectively.

Effects of Compaction

The layered compaction effect is illustrated in Figure 9. When a compaction effort is applied on the top of a soil layer, the highest unit weight is expected at the top of the layer while it decreases along the depth. Contrary to this, at the top of the layer, enough confinement is not found to develop a high unit weight due to the compaction. This results in lower unit weight in the top and bottom of the soil layer. In addition to this effect, compaction efforts applied on top layers may also be distributed in the already compacted bottom layers as shown in Figure 9. Therefore, change in the unit weight of the layers can be expected due to the effect of the compaction. Figure 9 illustrates logically this behavior in a soil sample. Variation in the unit weight in a sample along the depth may be reflected in the cone test results.

Miniature CPT

In order to verify the homogeneity of the compacted soil sample and repeatability of the miniature cone penetration test results, five locations were selected for cone tests. Averaging the cone tip resistance along the depth of soil sample was performed by excluding a thickness, used for compacting a soil layer, of about 0.125 m from the top and 0.25 m from the bottom of the sample. This procedure avoids the end effects of the soil sample. It is observed that the tip resistance varies with the depth of the soil sample. This is because the influence from the compaction of top layers may be expected on the previously compacted lower layers.

Table 3
Properties of the soils used in the laboratory cone test

Property	PRF-Silt	Sand
Passing sieve #200 (%)	39	2
Clay (%)	9	0
Silt (%)	30	2
Organic content (%)	NA	NA
Liquid limit (LL) (%)	NP	NP
Plastic limit (PL) (%)	NP	NP
Plasticity index (PI)	NP	NP
Specific gravity (G_s)	2.69	2.67
Angle of internal friction (ϕ) (^{o})	28.0	28.0
Optimum water content (w_{opt}) (%)	15.2	8.1
Maximum dry unit weight (γ_{dmax}) (kN/m^3)	17.2	16.4
Soil classification (*USCS*)	SM (Silty sand)	SP (Poorly graded sand)
Soil classification (*AASHTO*)	A-4 (Sandy loam)	A-3 (Fine sand)

Legend: NA- not available and NP- non plastic

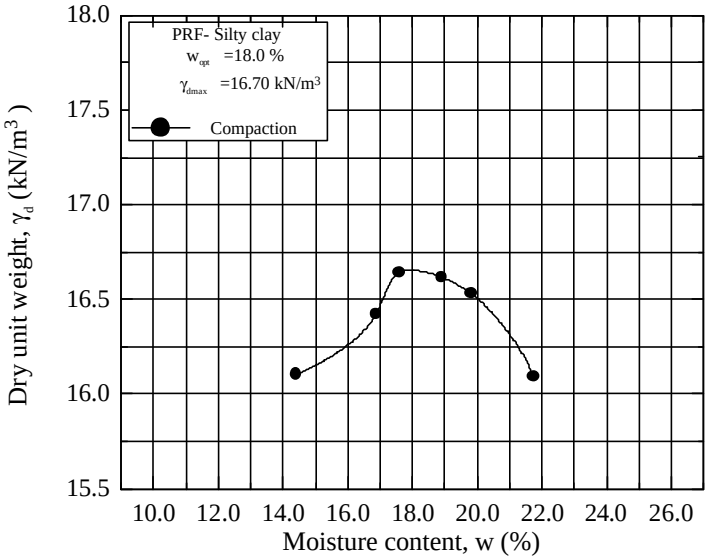

Figure 5
Moisture-unit weight relationship of silty clay

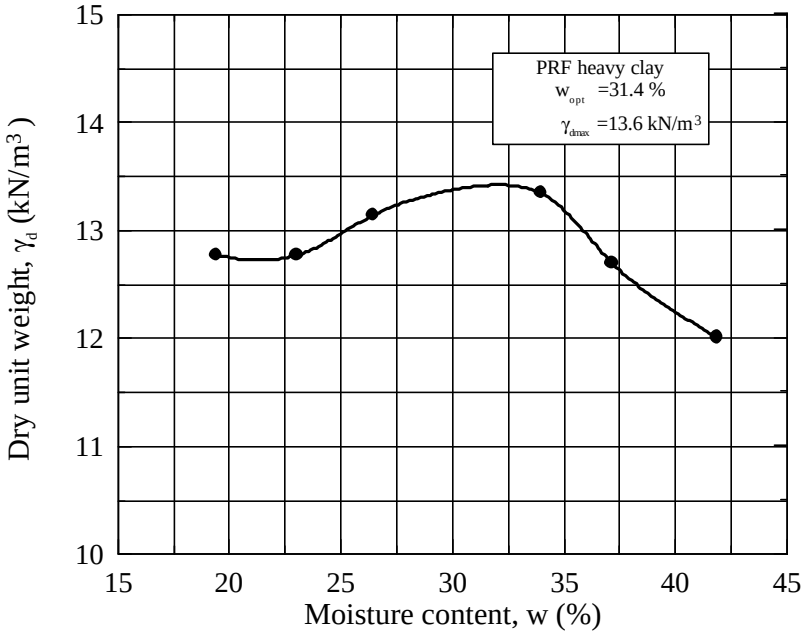

Figure 6
Moisture-unit weight relationship of heavy clay

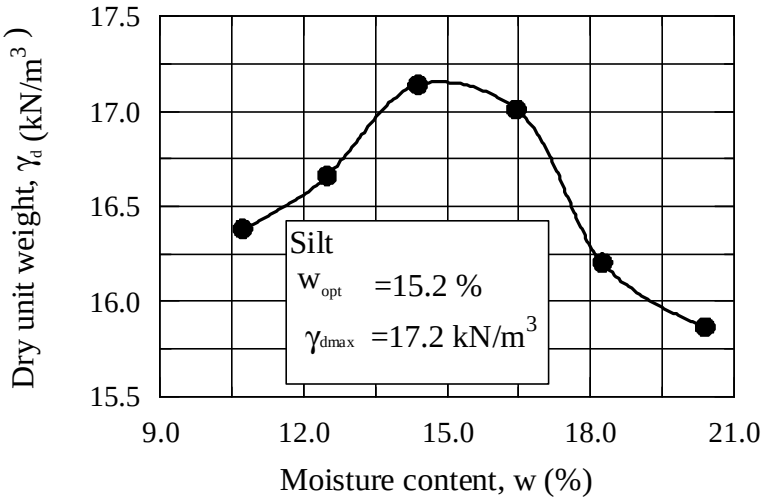

Figure 7
Moisture-unit weight relationship of silt

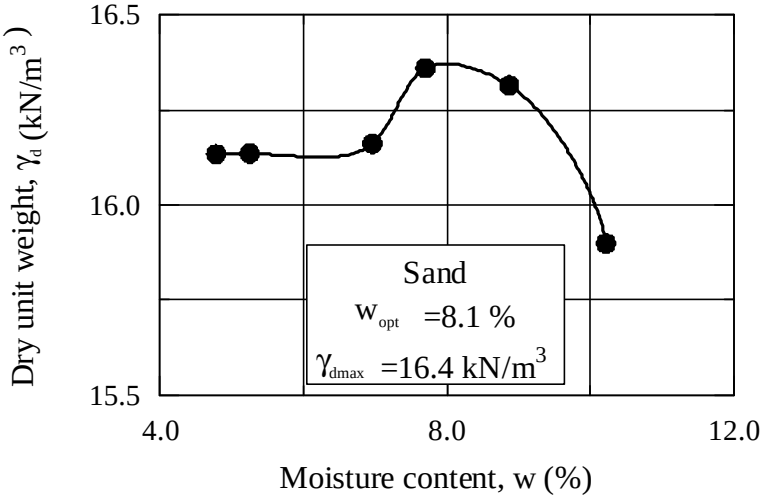

Figure 8
Moisture-unit weight relationship of sand

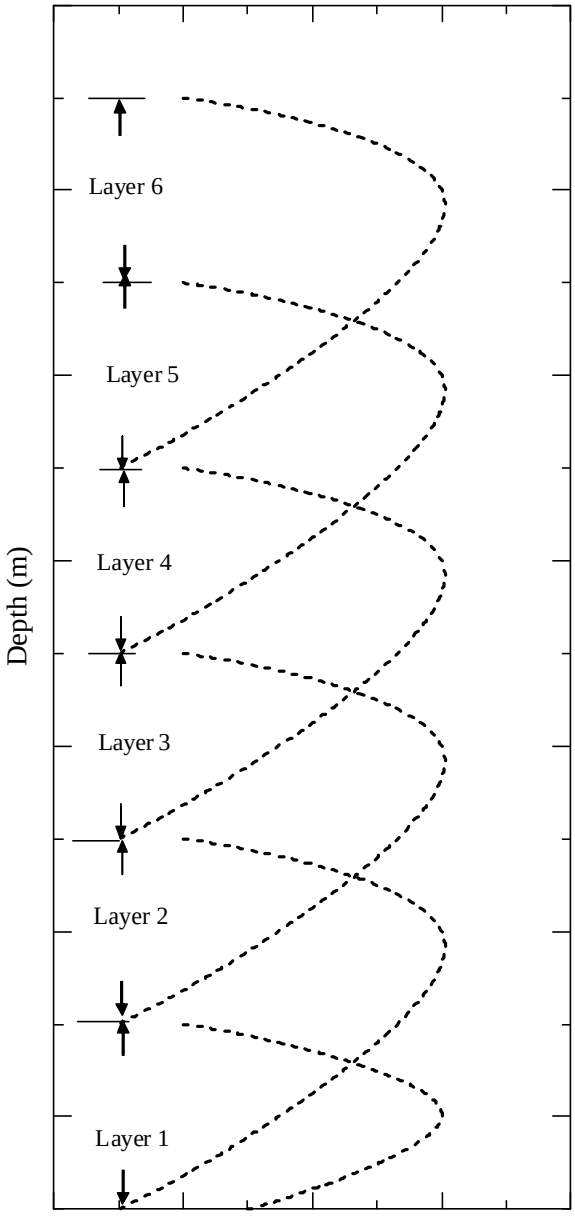

Figure 9
Effect of layered compaction

Figure 10 shows the laboratory cone penetration test results of silty clay at dry side. The variation in the cone tip resistance and sleeve friction along the depth of the sample is shown. The cone penetration test results of all five tests in a sample were considered from 0.125 m to 0.5 m to estimate the average tip resistance, sleeve friction, and coefficient of variation. The cone tip resistance of dry side showed an average value of 1.5 MPa with a standard deviation of 0.3 MPa. This result shows a variation of tip resistance in different compacted layers. The coefficient of variation is depicted in Figure 11. For the depth of data analysis, 0.125 m to 0.5 m, the average coefficient of variation of tip resistance for silty clay-dry side is 21 percent. Coefficient of variation for sleeve friction of silty clay-dry side is 7.7 percent. This variation in the cone test results is due to the effect of layered compaction.

Figure 12 presents the cone penetration test results for the soil prepared at the optimum moisture content point. The cone tip resistance along the depth of the sample is a result from the variation of the soil density along the depth as explained. Comparison of Figures 10 and 11 shows that tip resistance at the optimum sample is higher than that of the dry side. Figure 13 shows the coefficient of variation for cone tip resistance and sleeve friction for the soil sample tested at the at the optimum moisture content point. The average coefficient of variation of tip resistance for silty clay-optimum is 25 percent.

Due to the high sensitivity of the miniature cone penetrometer and its capability to identify thin soil layers, the above variation in the laboratory miniature cone penetration test results is expected. As shown in Figure 14, the lowest tip resistance was observed in the wet side soil sample. This implies that a combined effect of moisture content and dry unit weight exists on the tip resistance. Figure 15 shows the coefficient of variation at the wet side. For the depth of data analysis, 0.125 m to 0.5 m, average coefficient of variation of tip resistance for silty clay-wet side is 7 percent. These observations are common for all the four soils.

Figure 16 shows the cone penetration test results at the dry side of the heavy clay. The average tip resistance of heavy clay-dry side is 1.3 MPa. The average tip resistance of heavy clay-dry side is less than that of silty clay-dry side. This is due to the soft nature of heavy clay. As shown in Figure 17, for the range of data analysis, coefficient of variation of tip resistance for heavy clay-dry side, optimum, and wet side are 13, 7, and 23 percent.

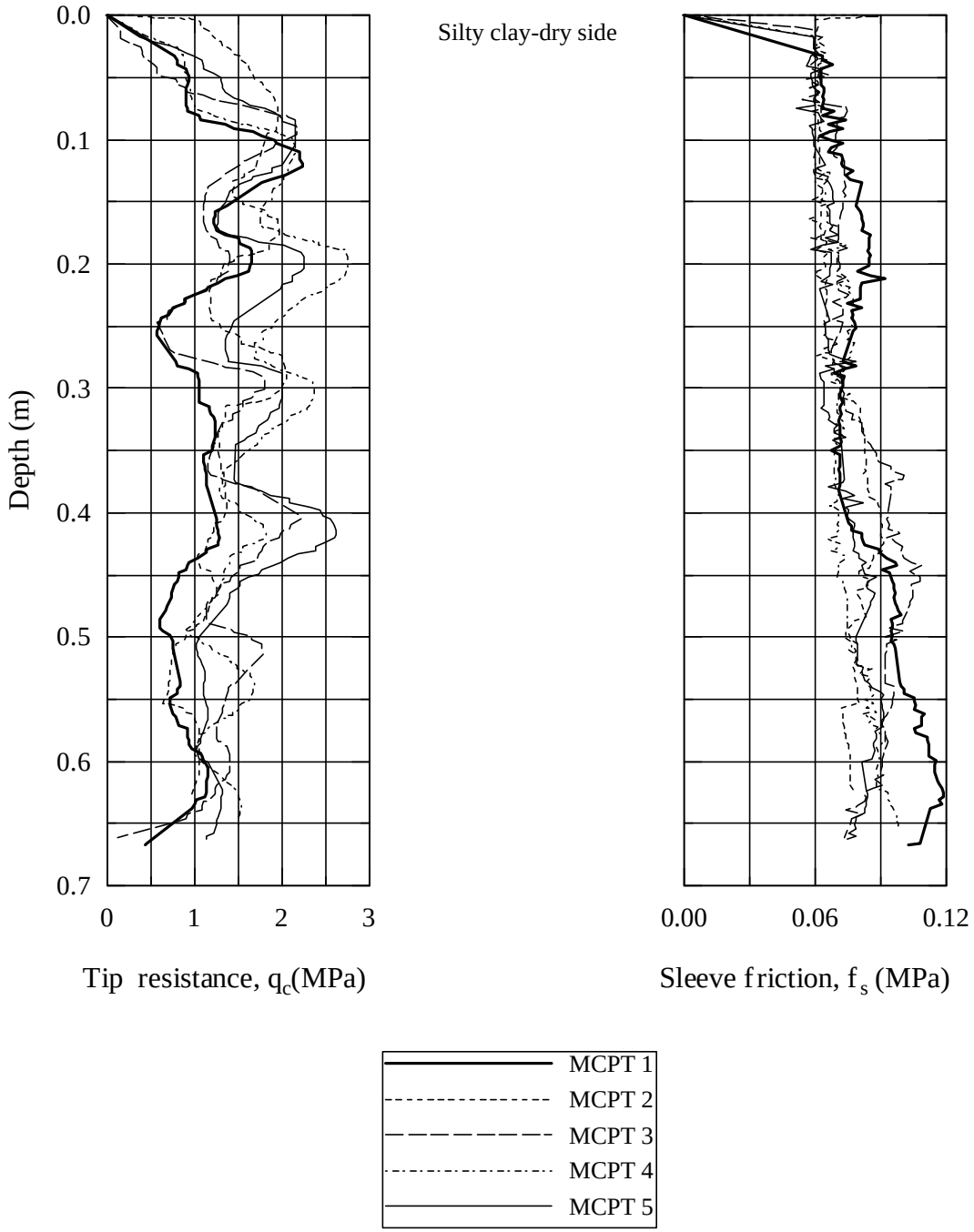

Figure 10
Laboratory cone penetration of silty clay at dry side

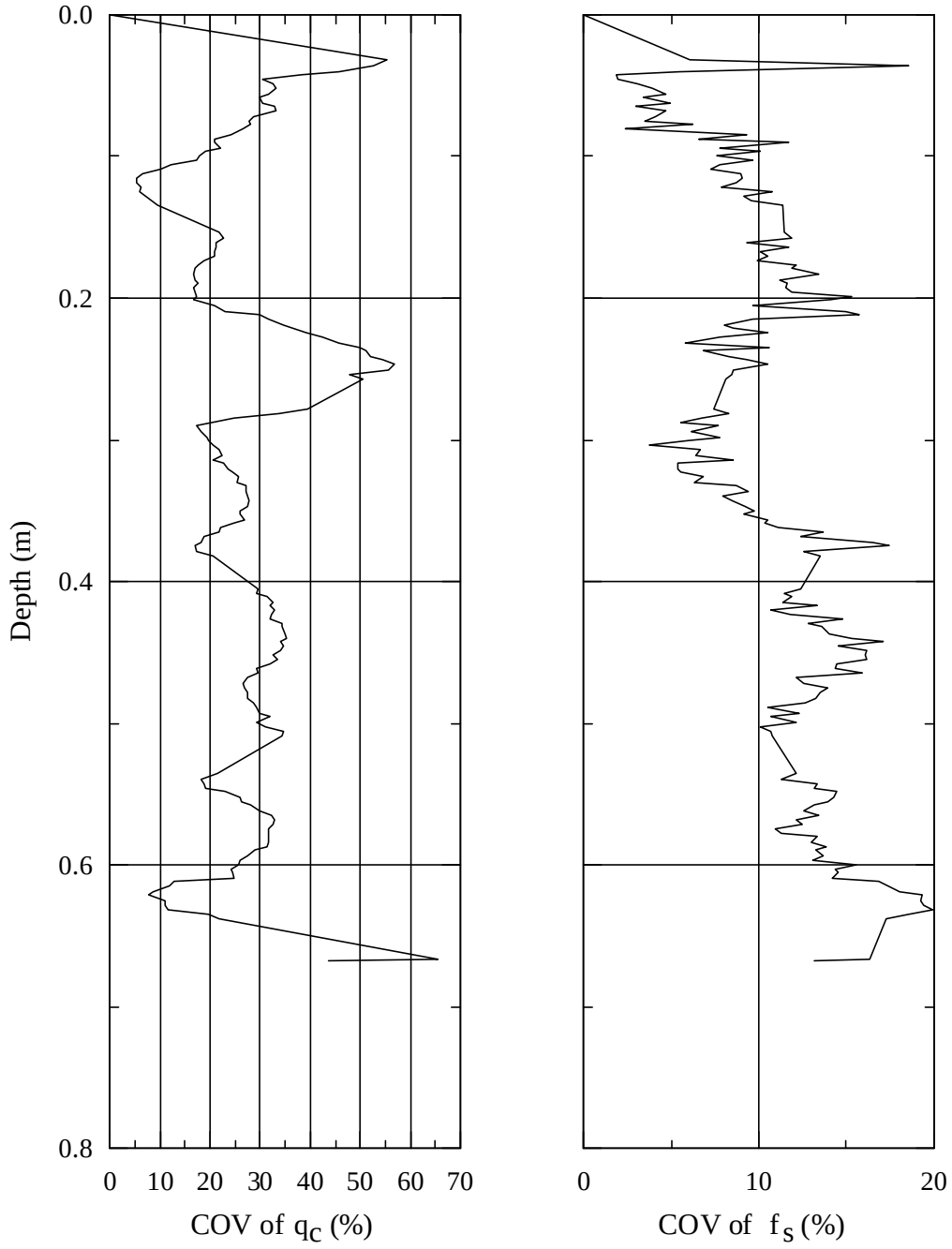

Figure 11
Coefficient of variation of laboratory cone penetration of silty clay at dry side

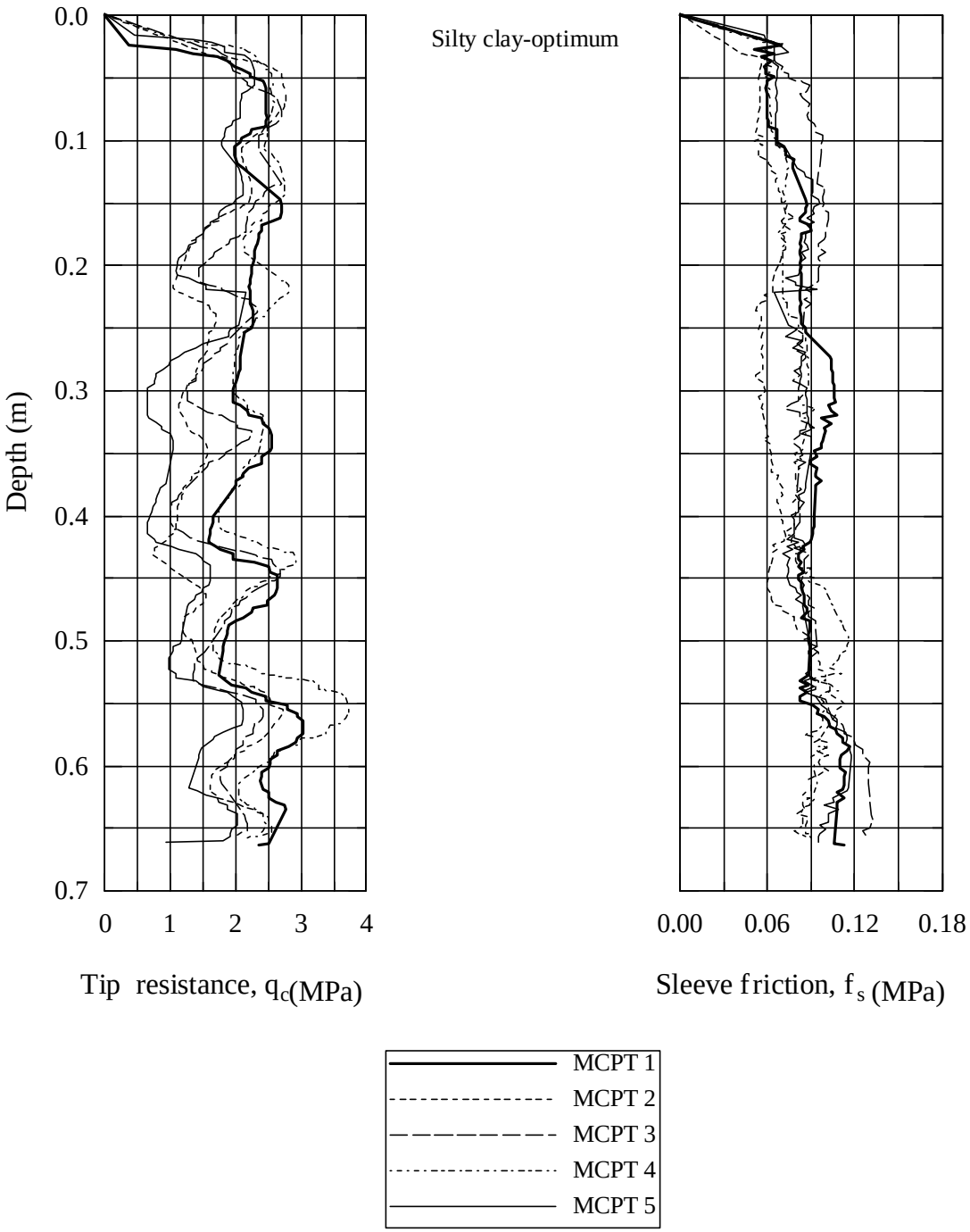

Figure 12
Laboratory cone penetration of silty clay at optimum

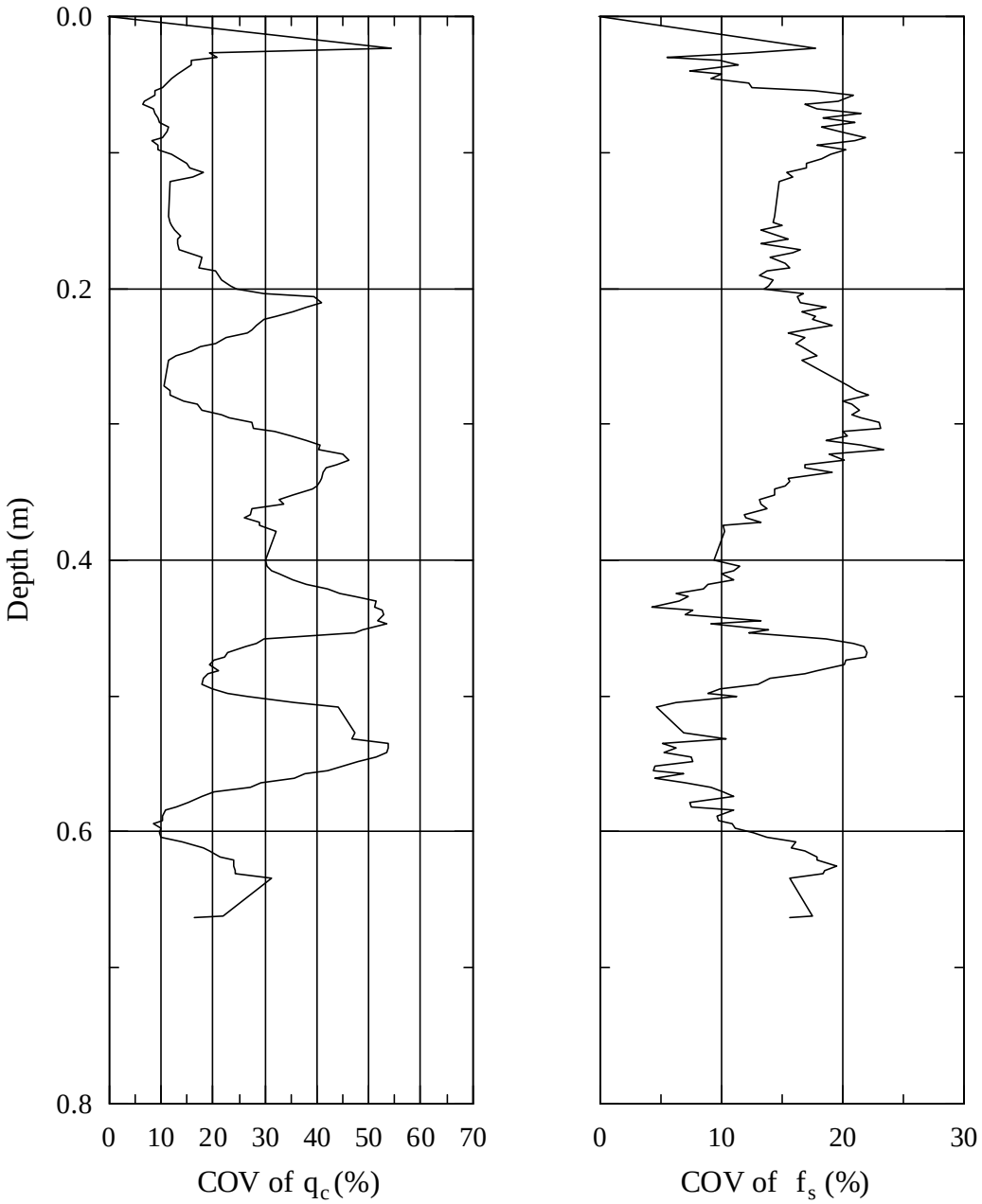

Figure 13
Coefficient of variation of laboratory cone penetration of silty clay at optimum

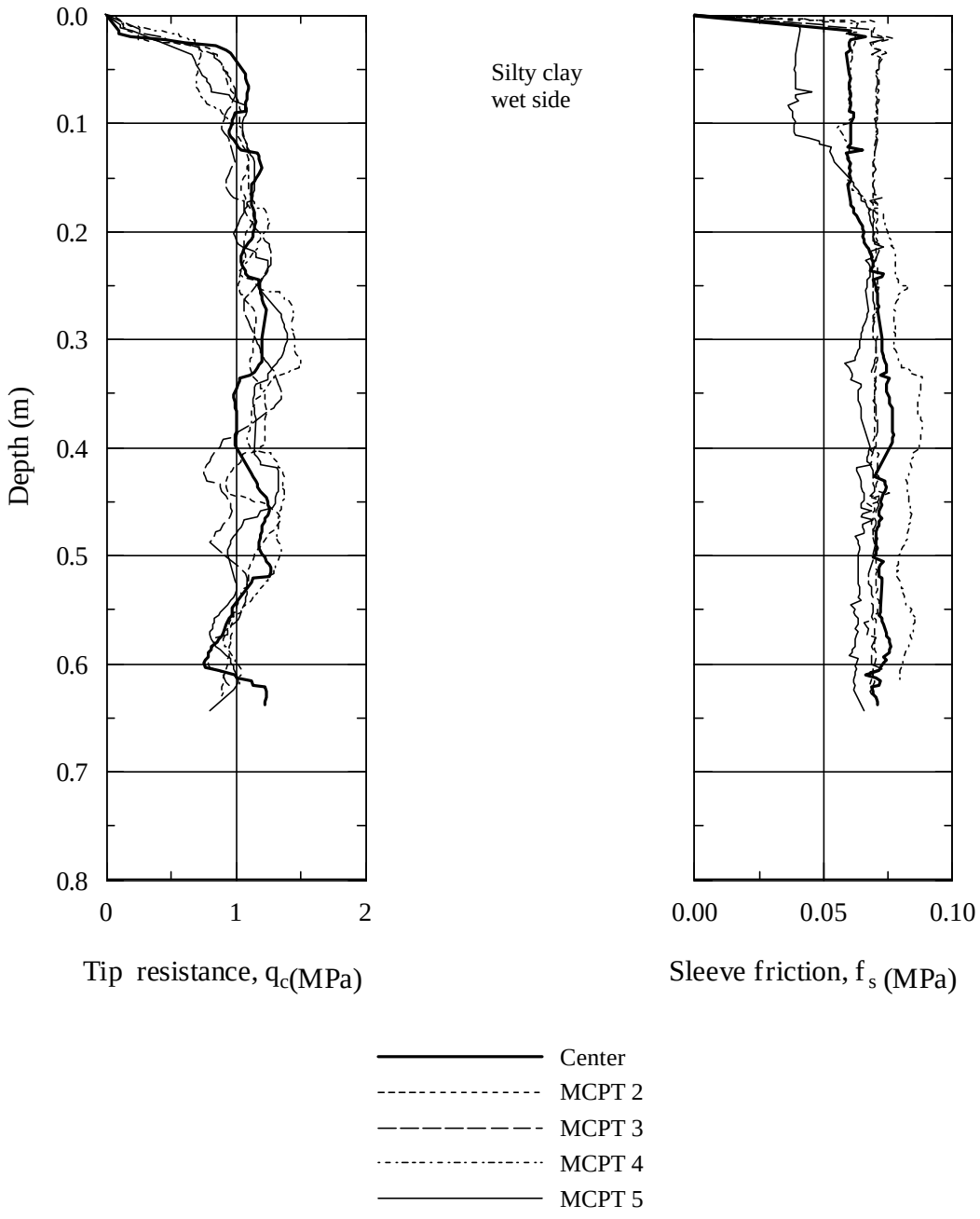

Figure 14
Laboratory cone penetration of silty clay at wet side

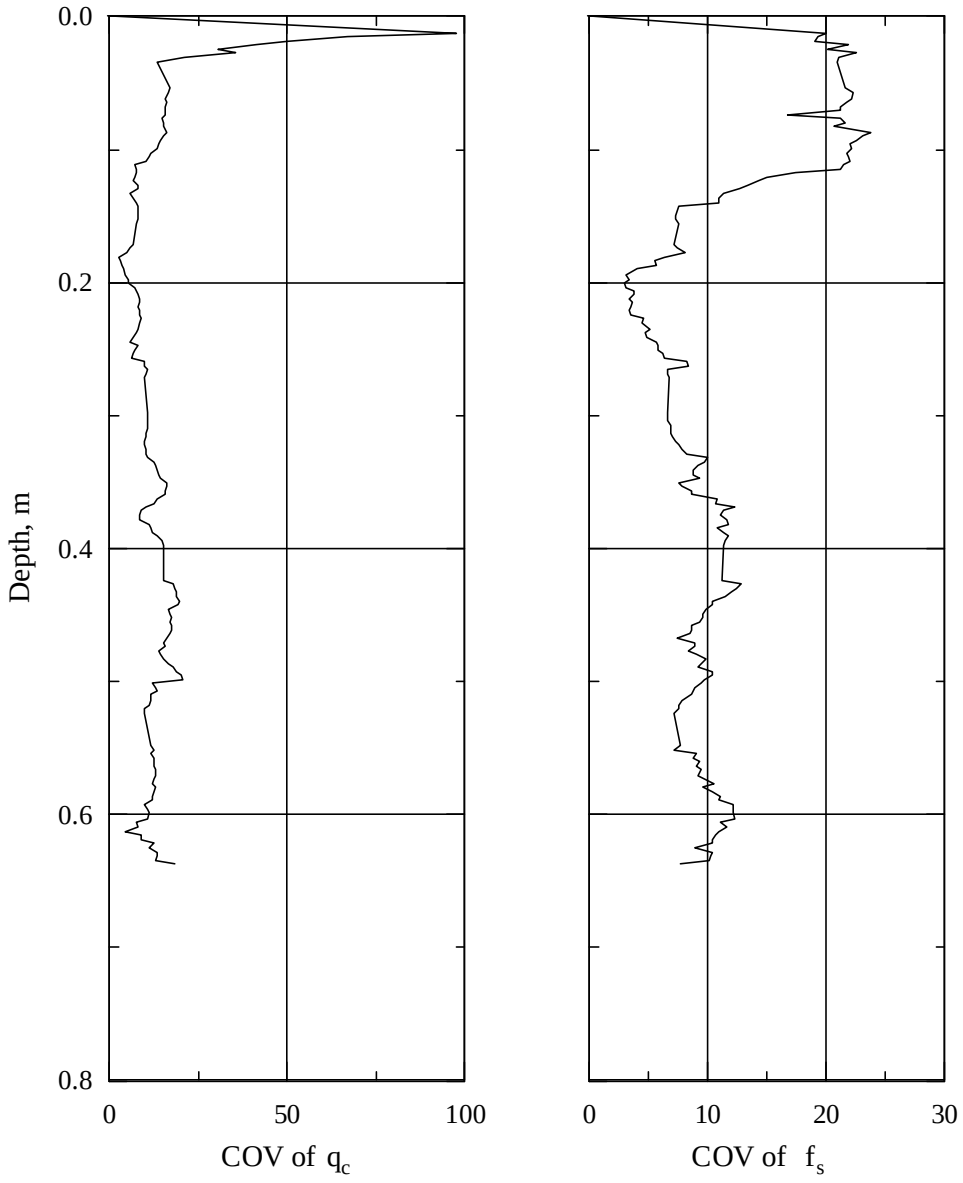

Figure 15
Coefficient of variation of laboratory cone penetration of silty clay at wet side

Figure 18 shows the cone penetration test results at the optimum of the heavy clay. The average tip resistance of heavy clay-optimum is 1.6 MPa. The average tip resistance of heavy clay-optimum is also less than that of silty clay-optimum. Coefficient of variation of tip resistance for heavy clay is 7 percent.

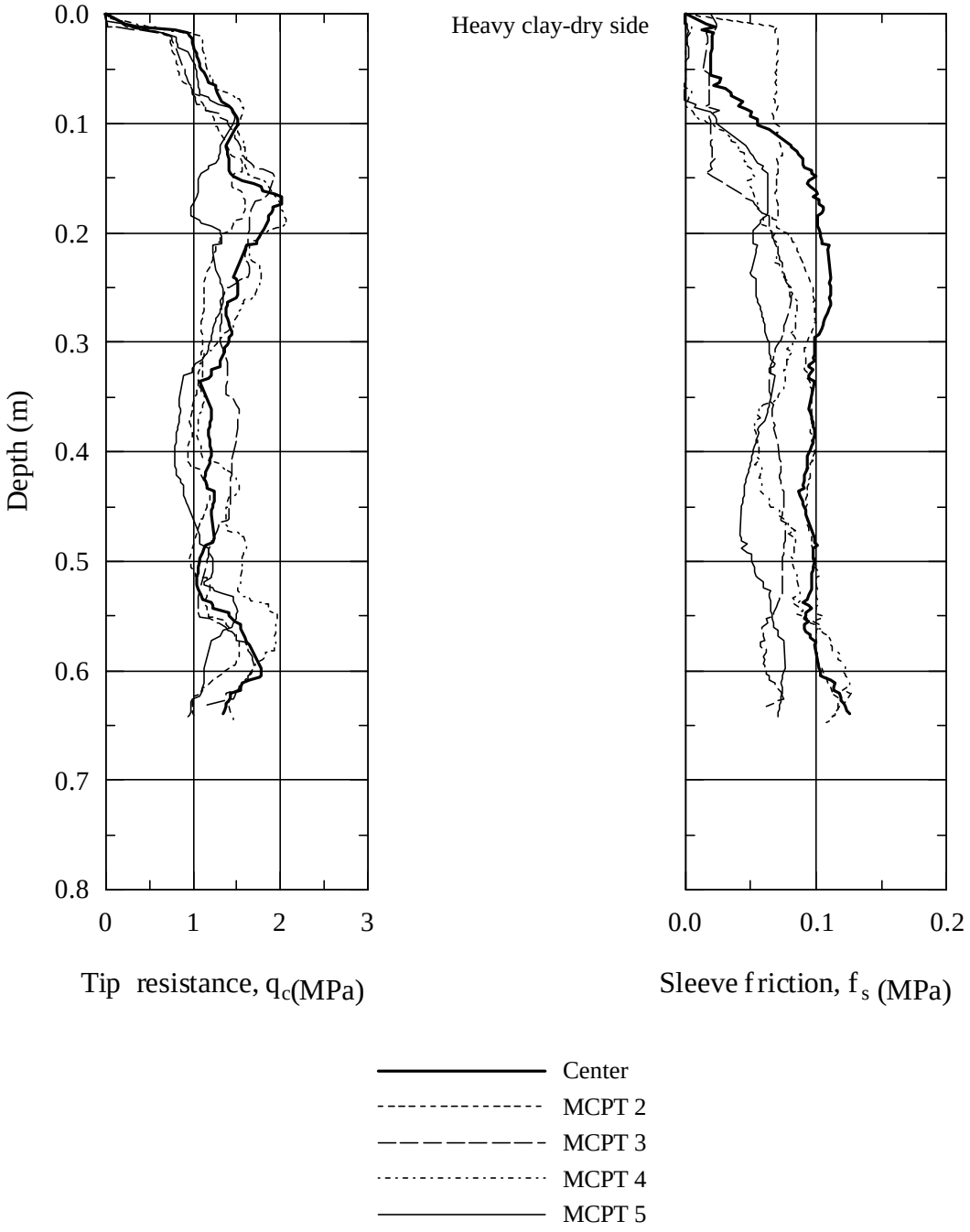

Figure 16
Laboratory cone penetration of heavy clay at dry side

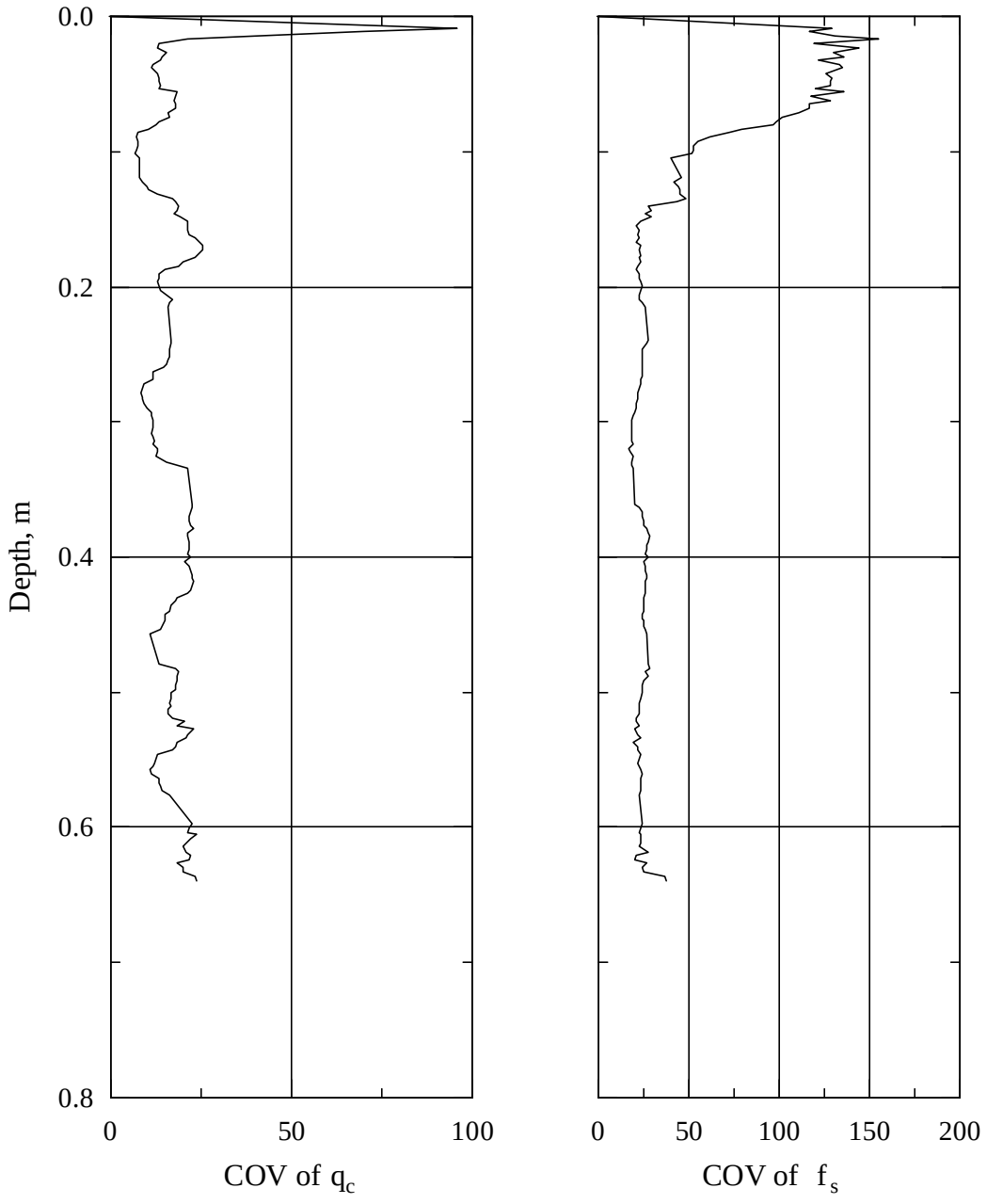

Figure 17
Coefficient of variation of laboratory cone penetration of heavy clay at dry side

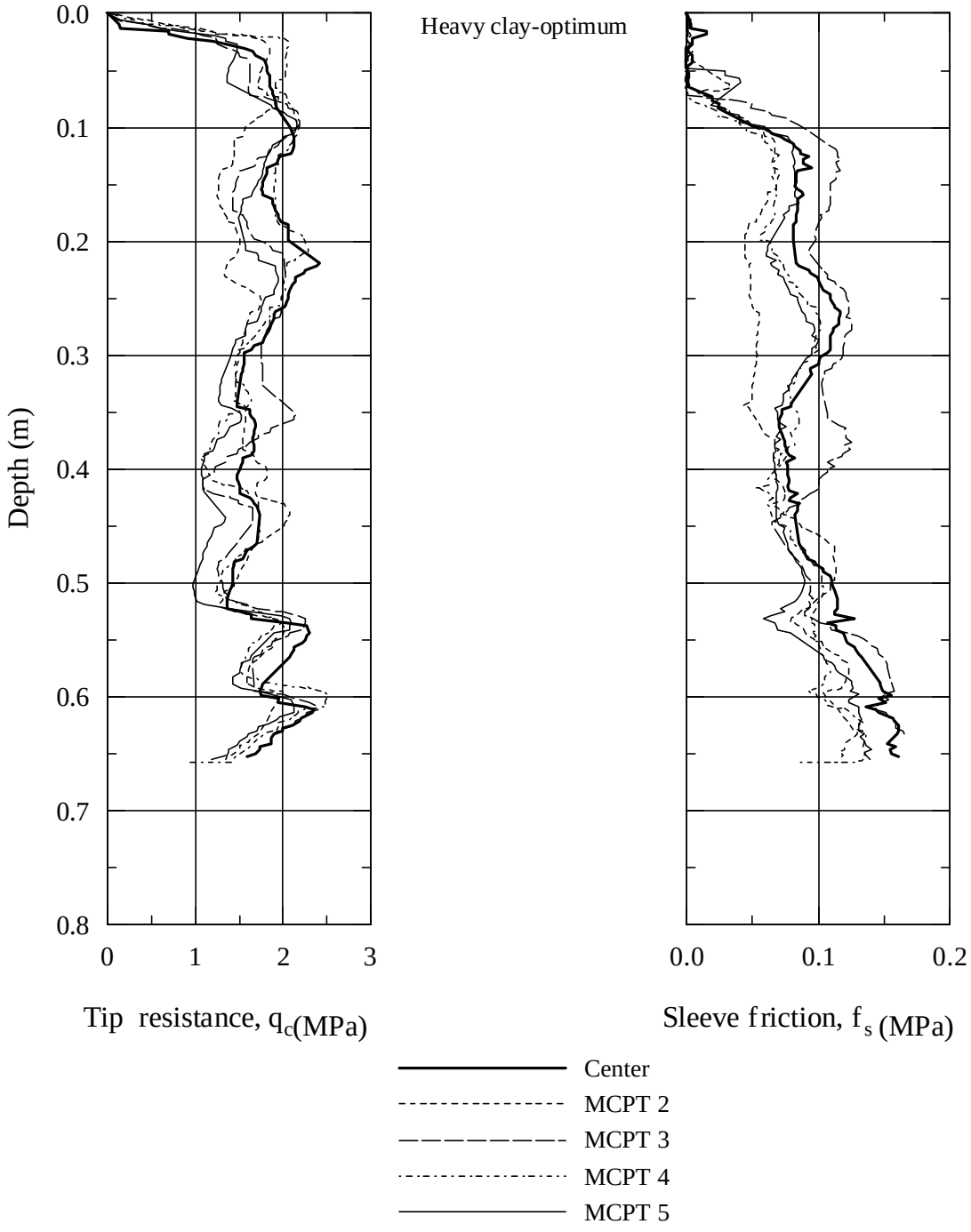

Figure 18
Laboratory cone penetration of heavy clay at optimum

Figure 19 presents the cone penetration test results at the wet side of the heavy clay. The cone test results for silt are depicted in Figures 20, 21, and 22. For the range of data analysis, coefficient of variation of tip resistance for silt dry side, optimum, and wet side are 15, 9, and 7 percent, respectively. Coefficient of variation of water content for silt dry side, optimum, and wet side are 4.0, 3.0, and 2.2 percent.

Cone tests for sand are depicted in Figures 23, 24, and 25. For the range of data analysis, coefficient of variation of tip resistance for sand dry side, optimum, and wet side are 16, 9, and 11 percent respectively. The observed sleeve friction was almost zero for silt and sand.

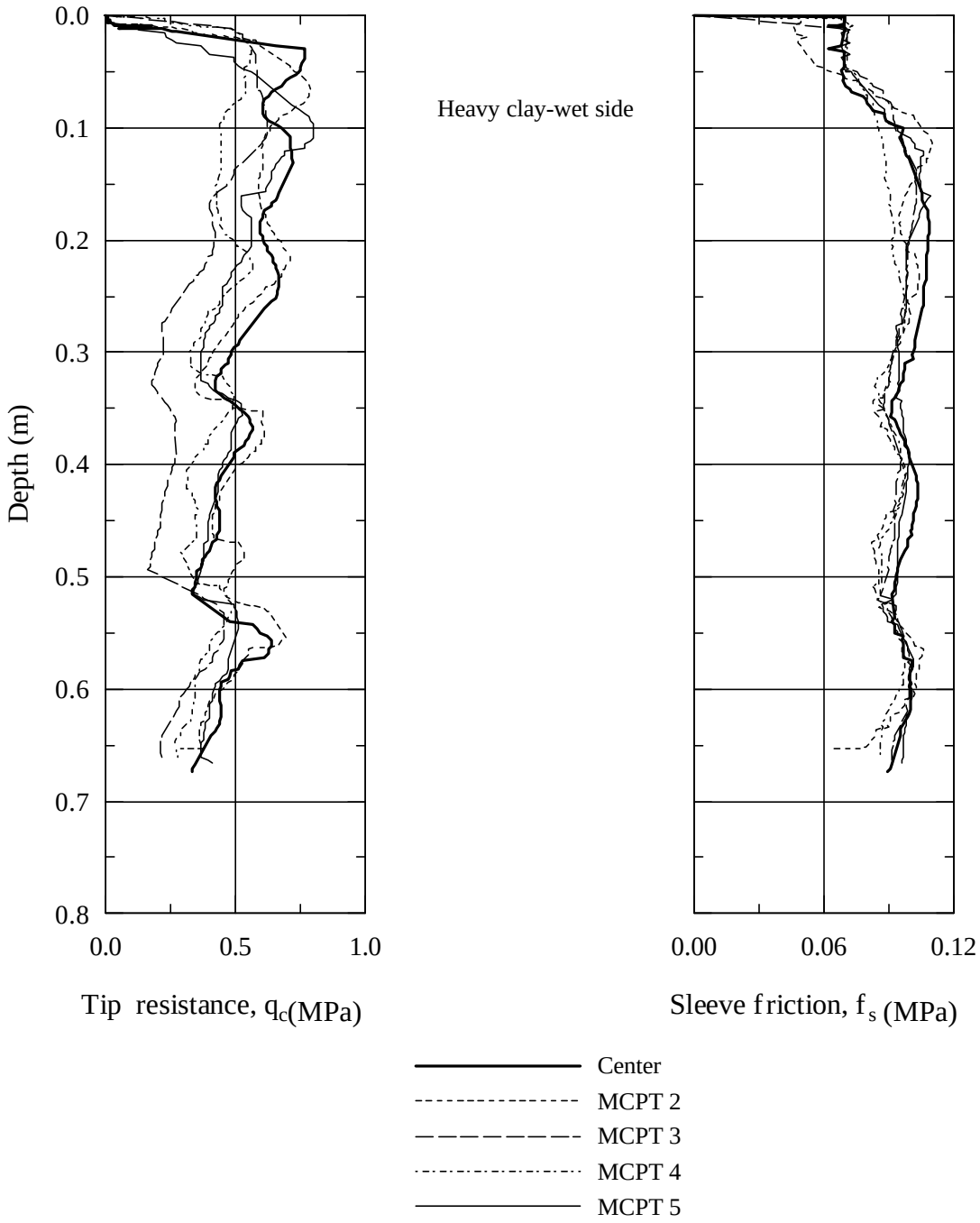

Figure 19
Laboratory cone penetration of heavy clay at wet side

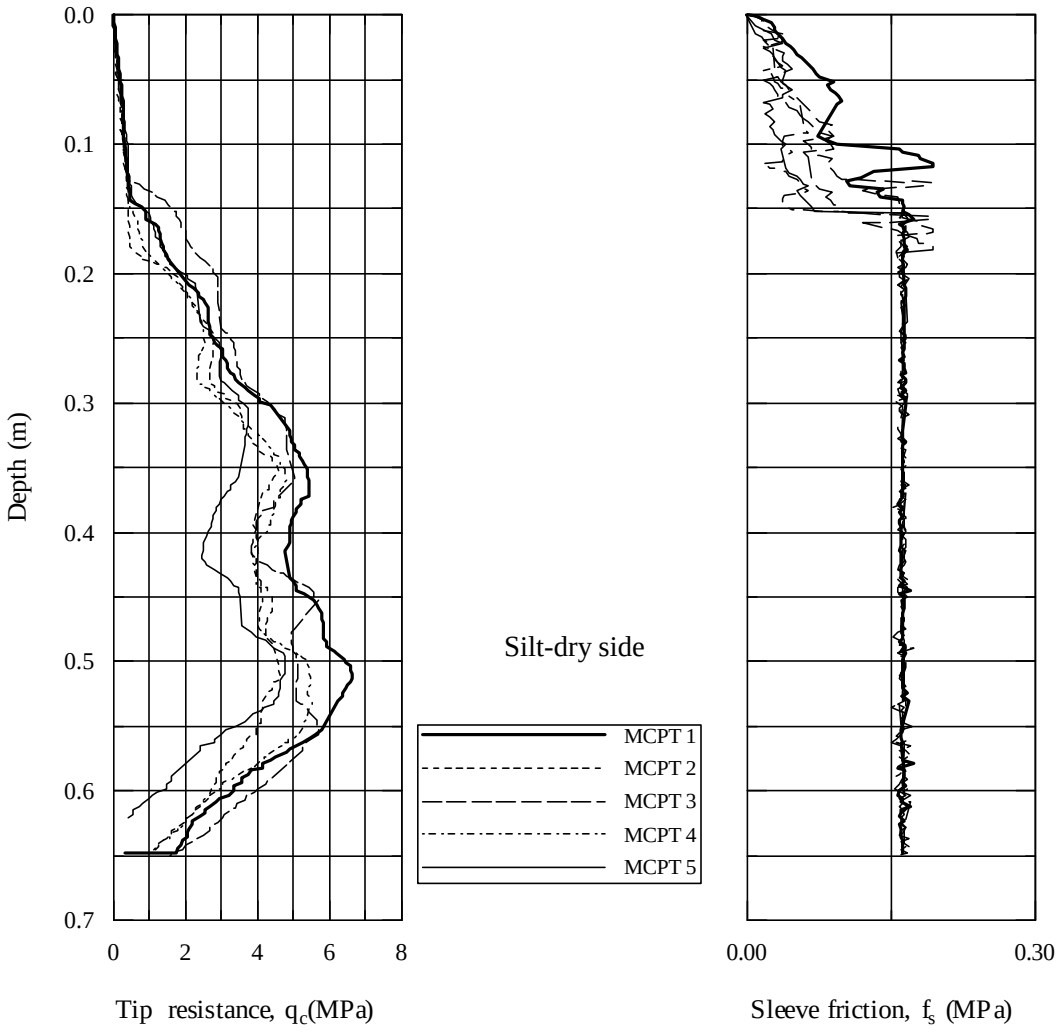

Figure 20

Laboratory cone penetration of silt at dry side

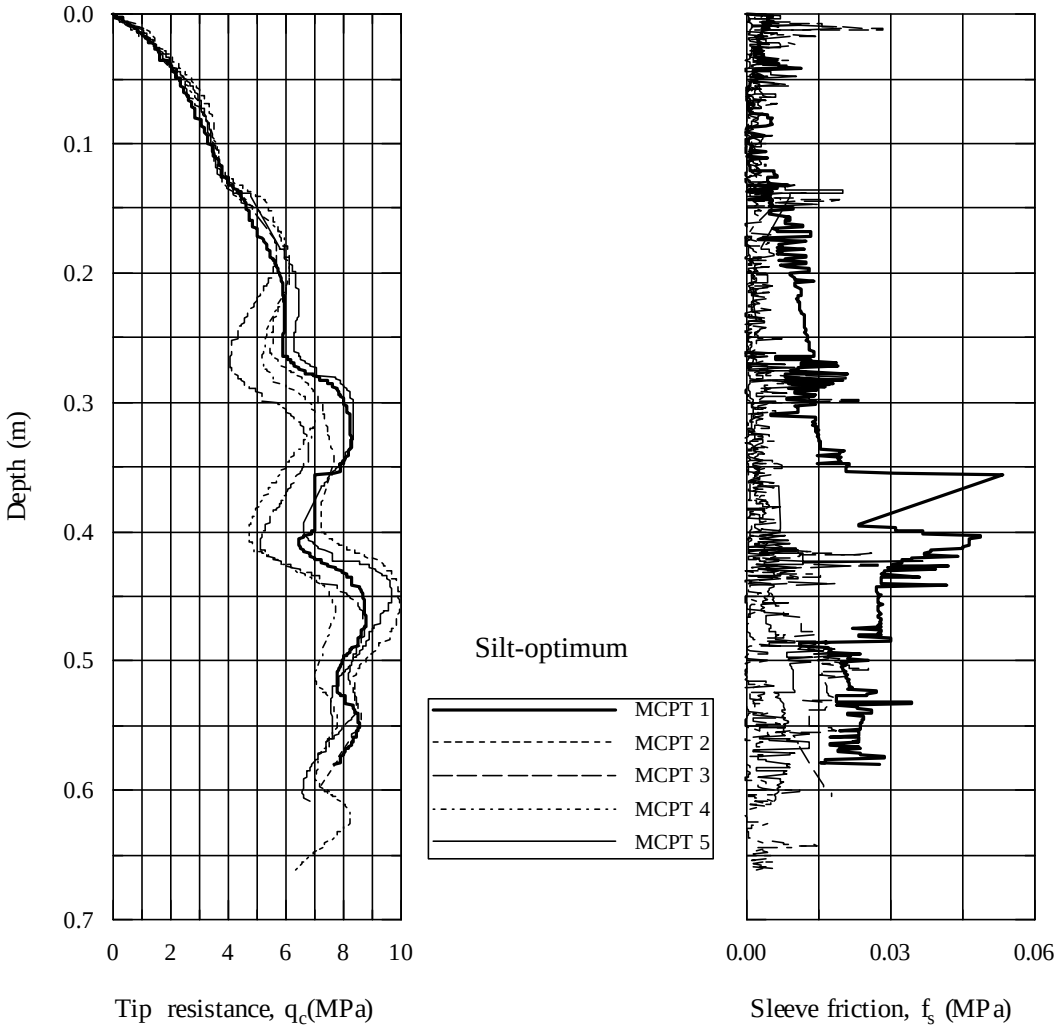

Figure 21

Laboratory cone penetration of silt at optimum

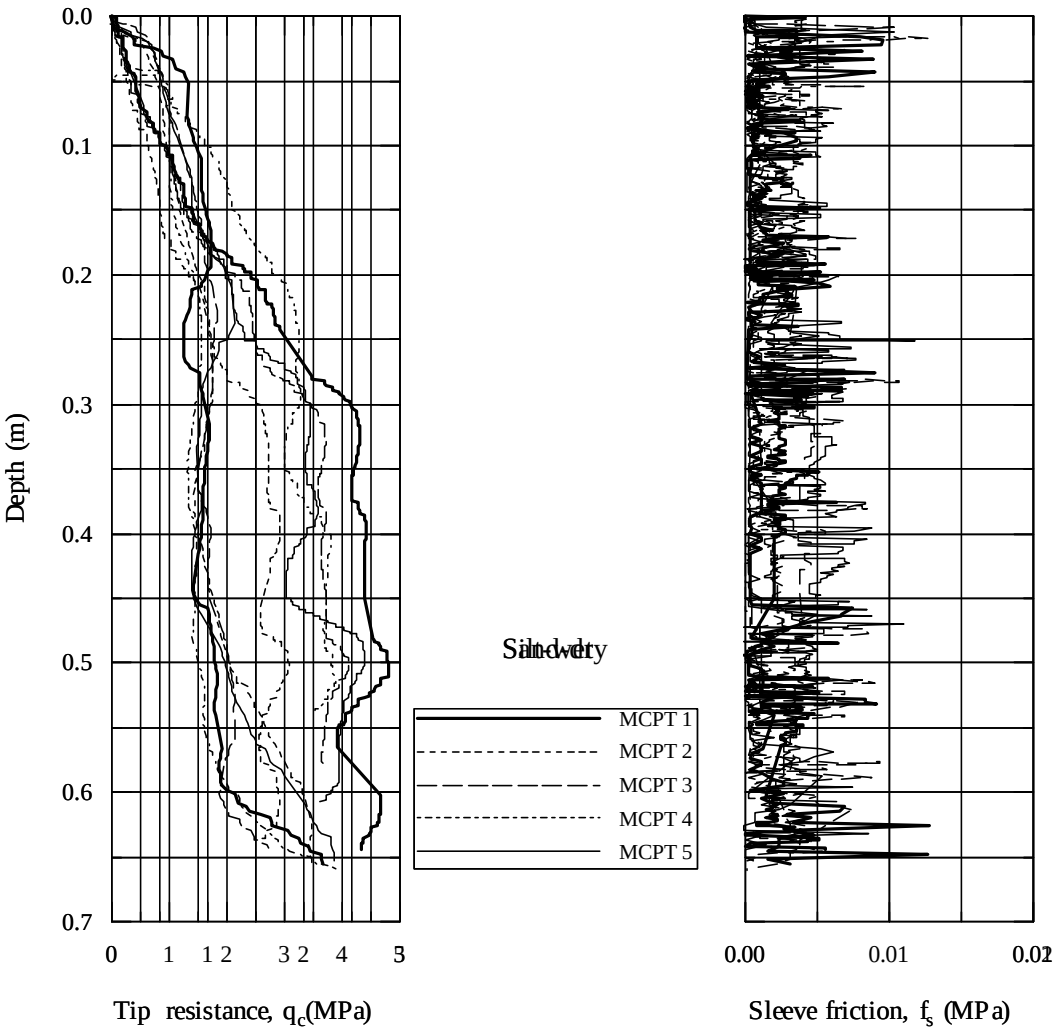

Figure 22

Laboratory cone penetration of silt at wet side

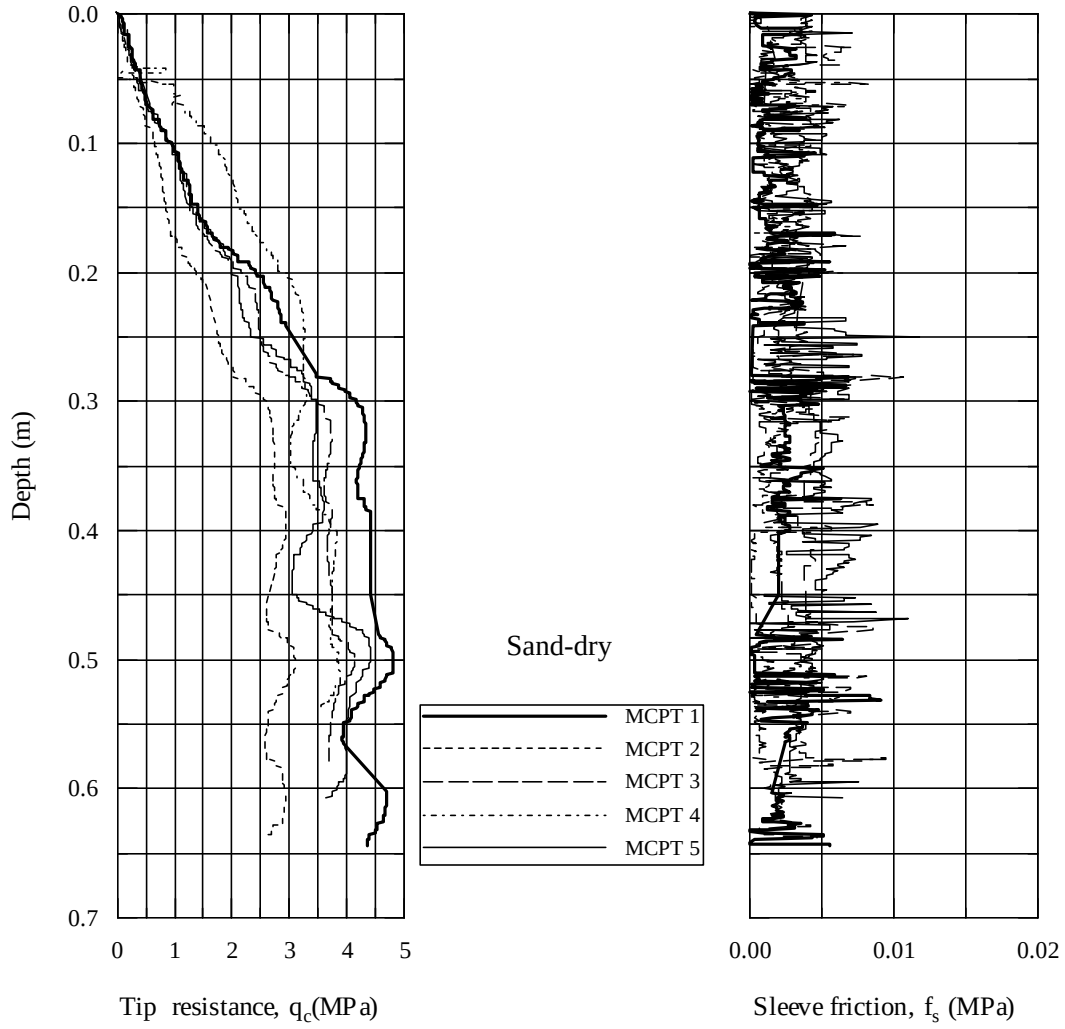

Figure 23
Laboratory cone penetration of sand at dry side

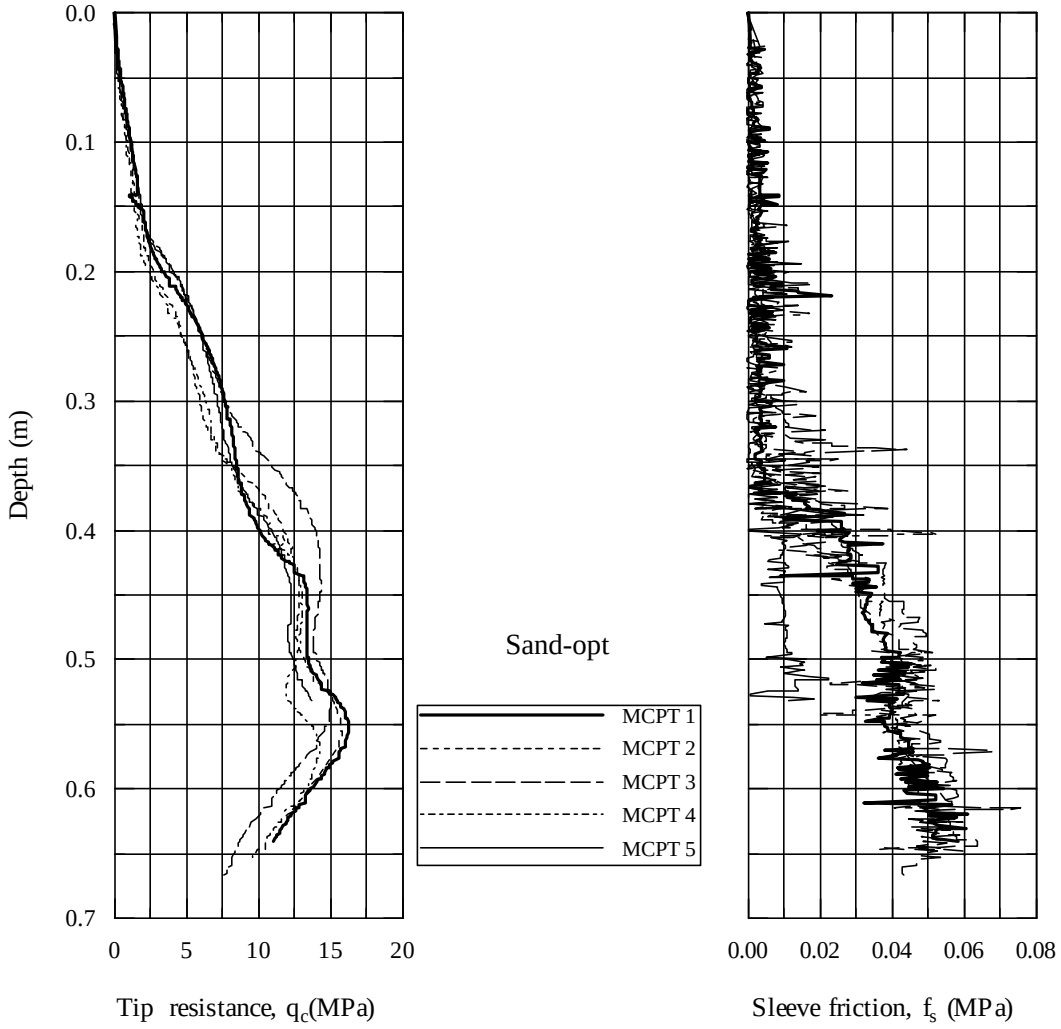

Figure 24

Laboratory cone penetration of sand at optimum

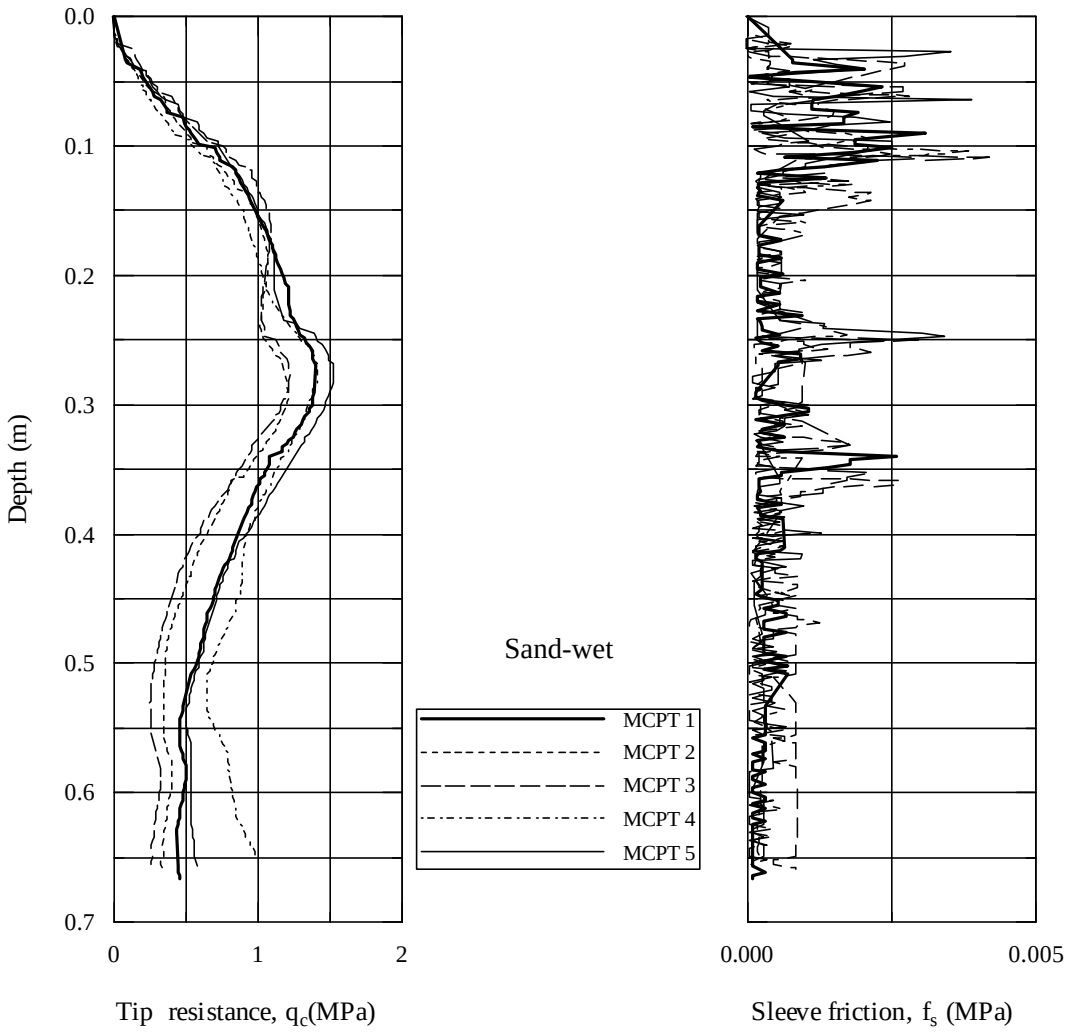

Figure 25
Laboratory cone penetration of sand at wet side

The Laboratory Resilient Modulus

A high resilient modulus for subgrade soil is desirable to obtain a resistance to deformation due to traffic loading. Figure 26 shows the resilient modulus test results for silty clay at dry side. As expected, the resilient modulus of silty clay decreases as deviator stress increases. The resilient modulus of silty clay is higher than that of heavy clay. The cone tip resistance follows the same pattern. This is due to the higher stiffness in silty clay and soft nature in heavy clay. At optimum, Figure 27, the highest resilient modulus is observed. The resilient modulus of silty clay dry side is greater than that of wet side, Figures 26 and 28. This is due to the high water content in the wet side. These observations are common for all the four soils. Figures 29, 30, and 31 present the resilient modulus of heavy clay dry side, optimum, and wet side respectively. Figures 32 and 33 show the resilient modulus test results for silt and sand on the dry side. As expected, the resilient modulus values of cohesionless soils increases with bulk stresses.

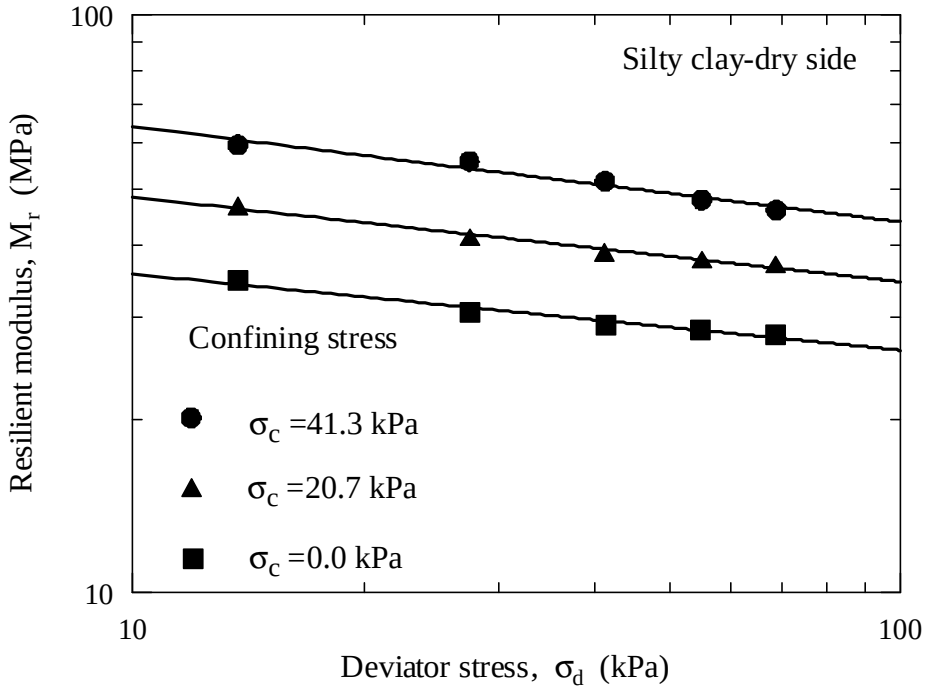

Figure 26
Resilient modulus of silty clay at dry side

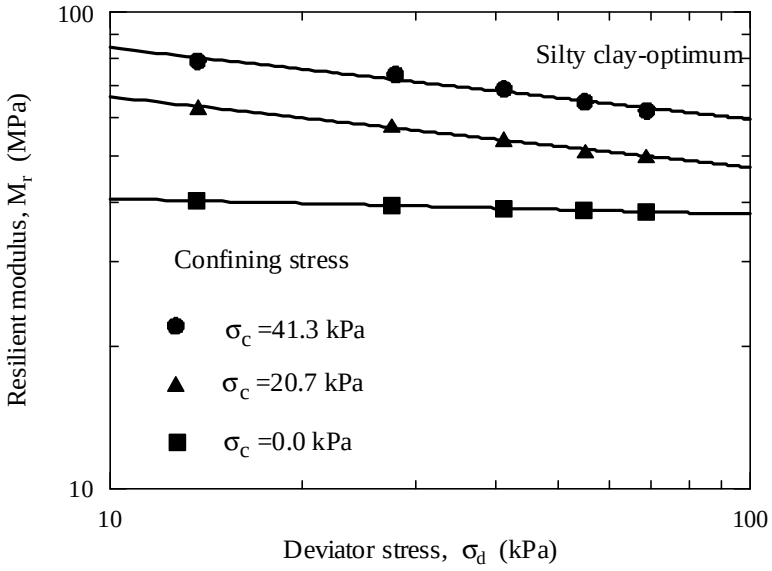

Figure 27
Resilient modulus of silty clay at optimum

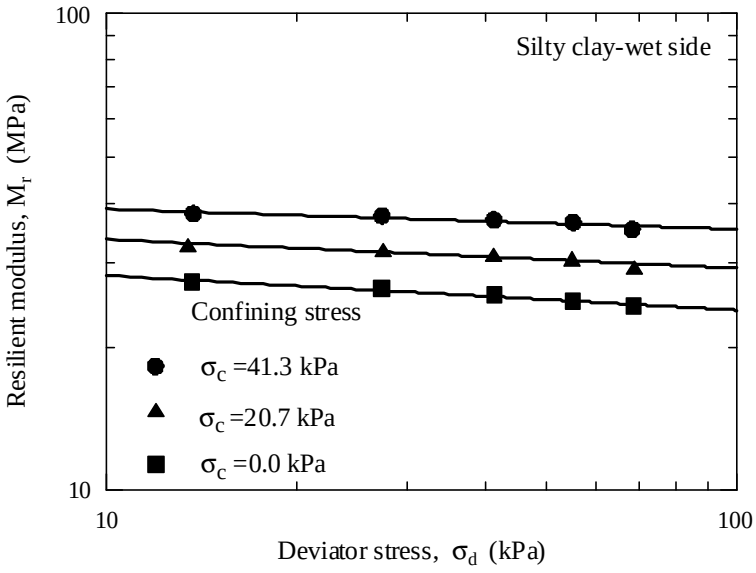

Figure 28
Resilient modulus of silty clay at wet side

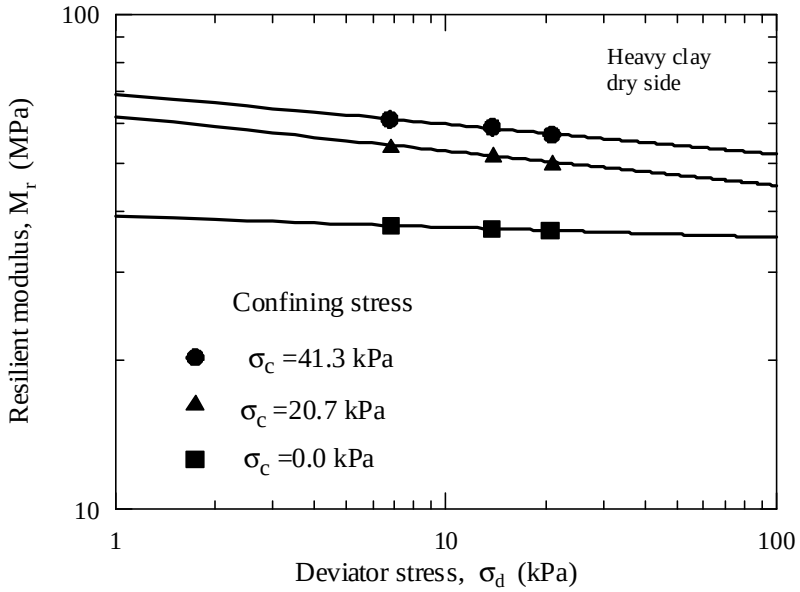

Figure 29
Resilient modulus of heavy clay at dry side

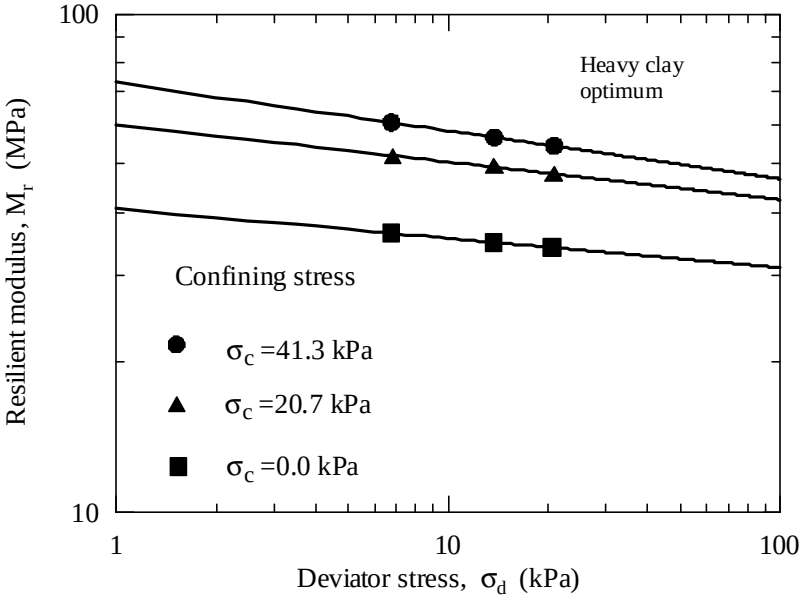

Figure 30
Resilient modulus of heavy clay at optimum

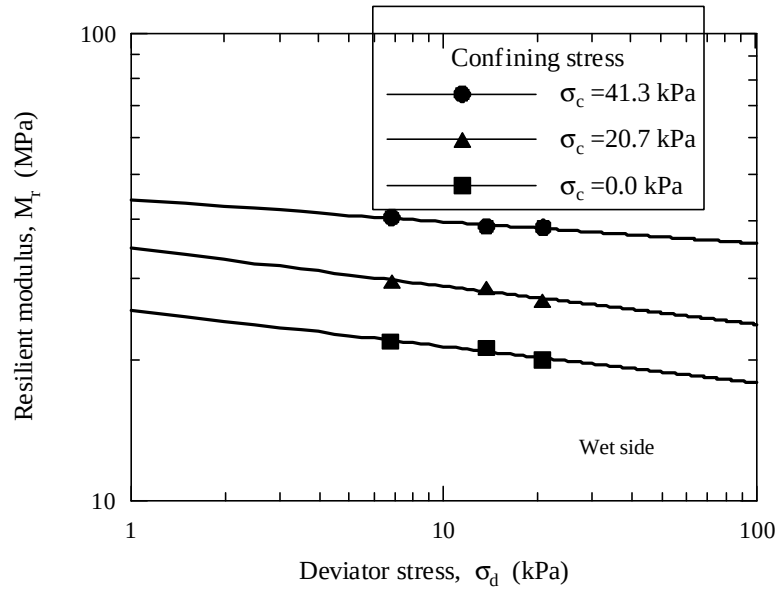

Figure 31
Resilient modulus of heavy clay at wet side

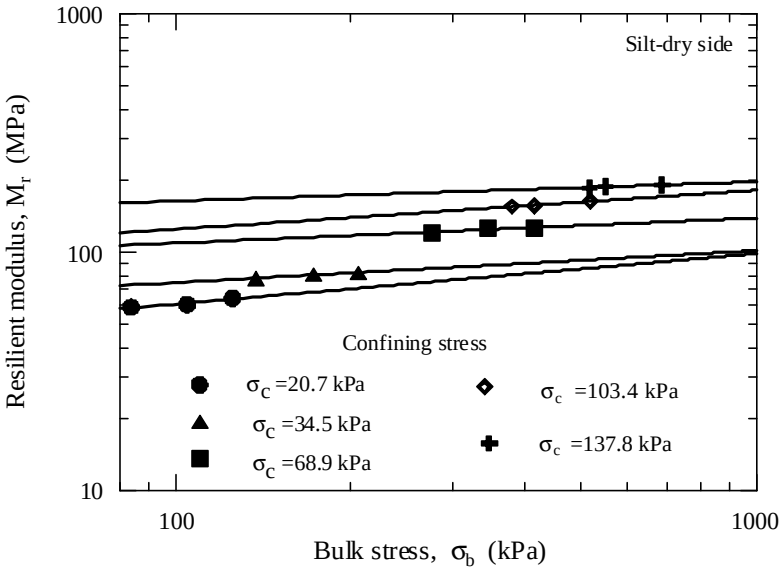

Figure 32
Resilient modulus of silt at dry side

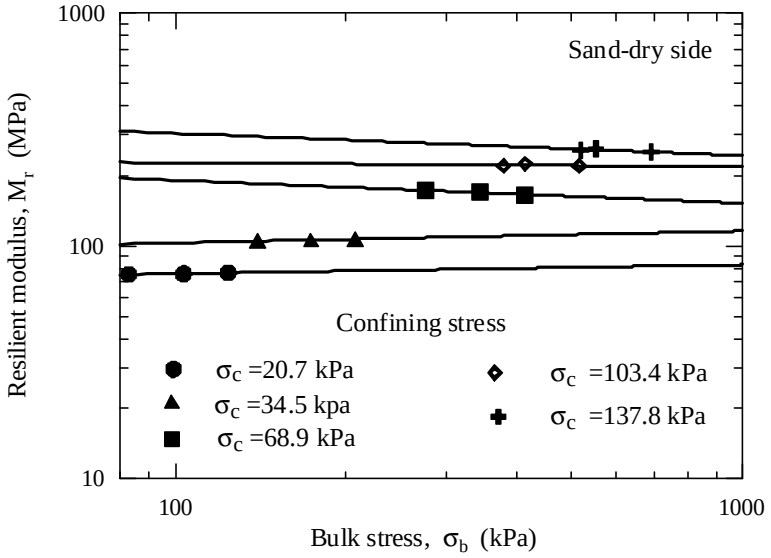

Figure 33
Resilient modulus of sand at dry side

Effect of Moisture Content and Unit Weight on Resilient Modulus

After cone penetration tests were completed, the soil sample was subjected to the moisture content and unit weight tests at different depths. For fine-grained soils and silt, the unit weight was estimated by using the sand cone test (LA-DOTD TR 401-95). Along the depth of the soil sample, moisture contents were also obtained.

Moisture content, determined along the depth of soil sample of silty clay-dry side, showed an average value of 14.2 percent, standard deviation of 0.3 percent, and coefficient of variation of 1.8 percent against the designed moisture content of 14.4 percent. Coefficient of variation of moisture content for silty clay dry side, optimum, and wet side are 1.8, 1.7, and 1.5 percent, respectively. Coefficient of variation of water content for heavy clay dry side, optimum, and wet side are 4.4, 2.2, and 1.3 percent respectively. Coefficient of variation of water content for sand dry side, optimum, and wet side are 1.6, 3.7, and 5.8 percent.

Dry unit weight determined along the soil sample depth of silty clay-dry side showed an average value of 15.9 kN/m^3, standard deviation of 0.2 kN/m^3, and coefficient of variation of 1.2 percent against the designed unit weight 16.1 kN/m^3. Coefficient of variation of dry unit

weight for silty clay dry side, optimum, and wet side are 1.2, 2.0, and 1.2 percent, respectively. Coefficient of variation of dry unit weight for heavy clay dry side, optimum, and wet side are 5.0, 2.8, and 2.8 percent respectively.

Coefficient of variation of dry unit weight for silt dry side, optimum, and wet side are 2.4, 7.6, and 3.8 percent. Coefficient of variation of dry unit weight for sand dry side, optimum, and wet side are 3.0, 6.2, and 2.2 percent. This type of variation can be expected due to the layered compaction effects. Among the four soil types, the maximum coefficient of variation for tip resistance, water content, and dry unit weight are 25, 6, and 5 percent, respectively.

Figures 34 and 35 depict the variation in the resilient modulus with the moisture content. In the wet side, as the moisture content increases effective deviator stress decreases and hence the resilient modulus decreases. In the wet side, soil fabric is dispersed whereas, in the dry side, soil is flocculated. Strength of the dispersed soil is less than that of flocculated soil. The resilient modulus is related to the strength of soil.

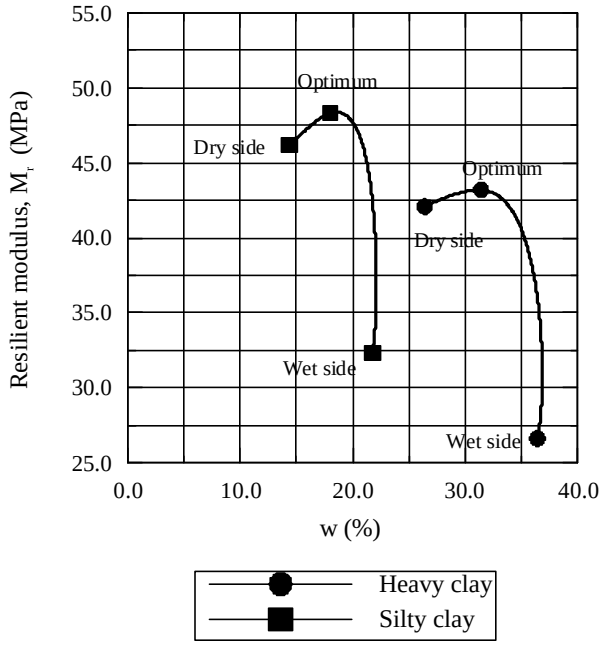

Figure 34
Variation in the resilient modulus with moisture content of fine-grained soil

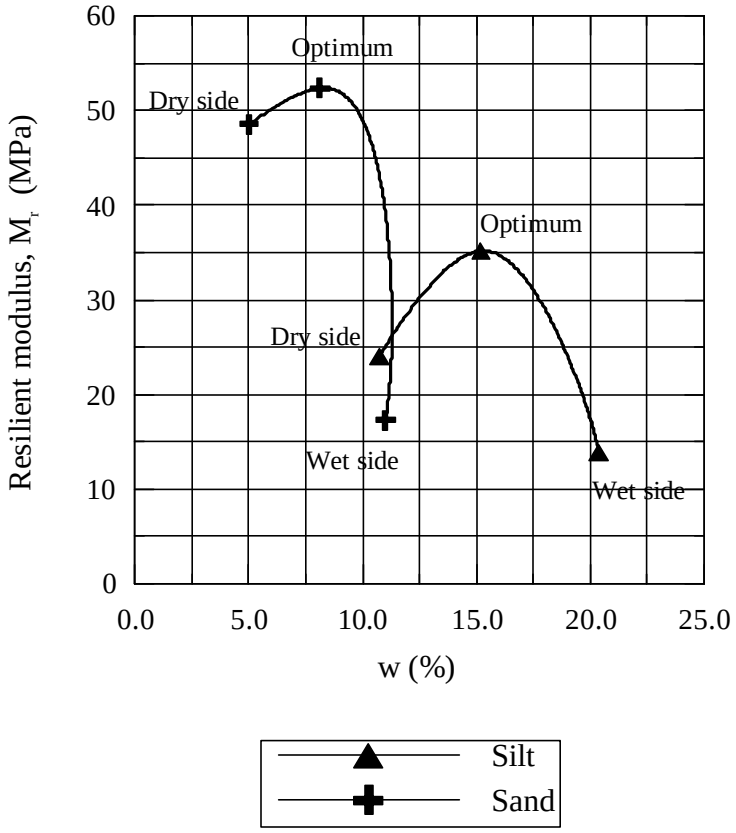

Figure 35
Variation in the resilient modulus with moisture content of coarse-grained soil

In silty clay, the change in the resilient modulus between the dry and wet sides was about 14 MPa for the change in moisture content of about 7 percent. In heavy clay, the change in the resilient modulus between the dry and wet sides was about 15 MPa for the change in moisture content of about 10 percent. This may result in the change in the overlay thickness of a pavement significantly, as discussed in the later part of this report. Figures 36 and 37 show the variation of resilient modulus with dry unit weight and moisture content. From the dry side to optimum, as the dry unit weight increases soil stiffens and hence the resilient modulus increases. From optimum to wet side the resilient modulus decreases with the increasing moisture content. It was observed that a combined effect of both moisture content and dry unit weight on the resilient modulus of soil exists. The maximum resilient modulus of each soil was observed at the optimum. The resilient modulus of dry side of each soil was greater than that of wet side at the same dry unit weight. Figures 38 and 39 show the same observations for the tip resistance.

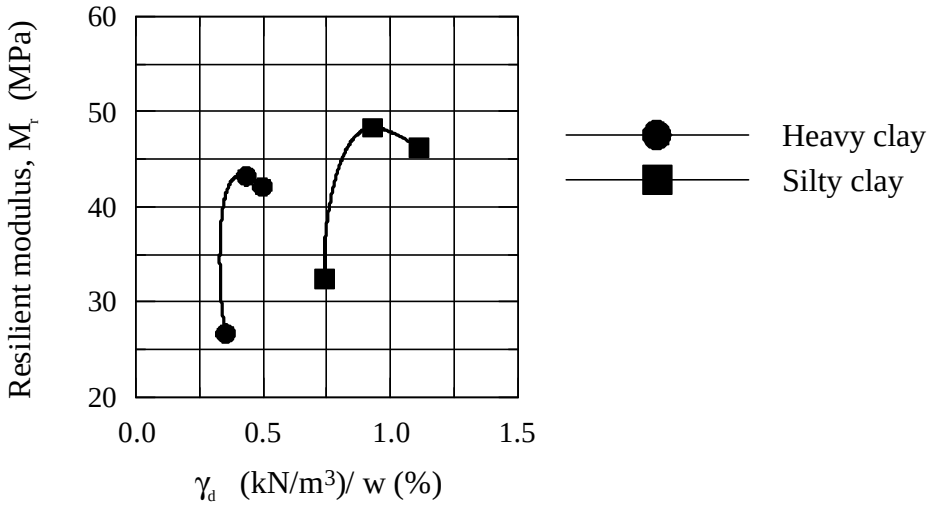

Figure 36
Variation of the moisture content, unit weight, and resilient modulus for fine-grained soil

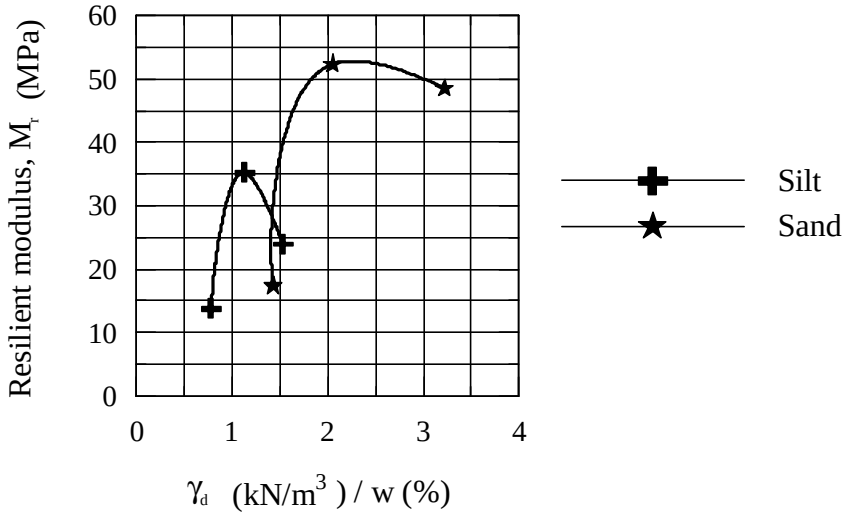

Figure 37
Variation of the moisture content, unit weight, and resilient modulus for coarse-grained soil

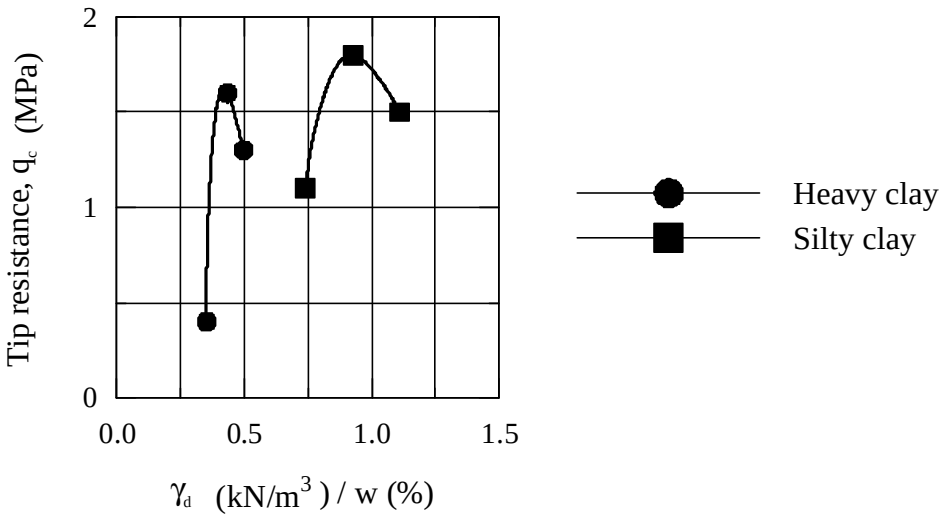

Figure 38
Variation of the moisture content, unit weight, and tip resistance for fine-grained soil

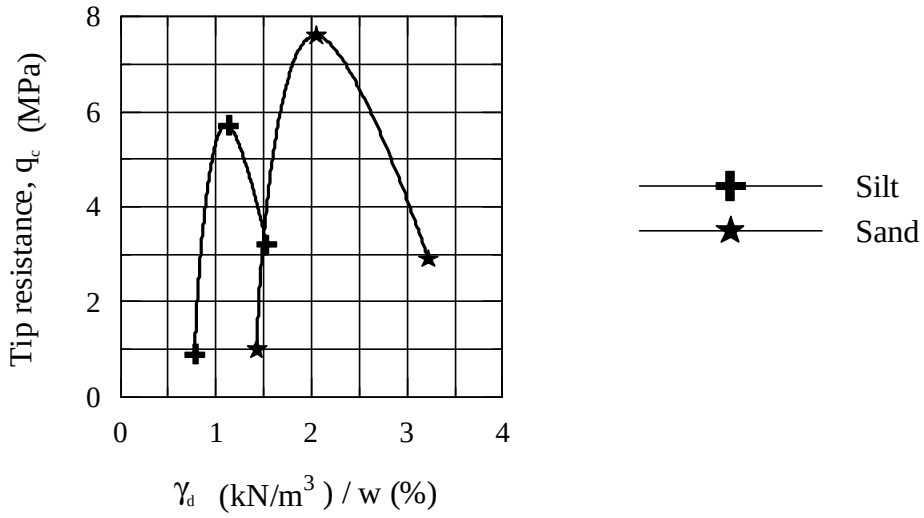

Figure 39
Variation of the moisture content, unit weight, and tip resistance for coarse-grained soil

Prediction of Resilient Modulus Using the CPT

Summary of the models developed during phase I of the research to predict resilient modulus of subgrade soils using the cone penetration test is described in the beginning of this report.

Tables 4 and 5 present the summary of the result of the laboratory testing program on the investigated soil. The data in Tables 4 and 5 are used to validate the prediction models developed in phase I of the research. As shown in Figure 40 and 41, the predicted and measured resilient modulus values are in agreement. These represent the resilient modulus determined for in-situ conditions. In order to consider the effect of traffic, the elastic properties of the pavement layers need to be considered. Table 6 presents the elastic properties. The modulus of elasticity (E) values were estimated from the laboratory repeated load triaxial testing. The Poisson's ratio (n) was assumed. The traffic stress models, developed during phase I of this research, were used to predict the resilient modulus of fine-grained soil. The predictions are presented in Figures 42 and 43. The results of the stress analysis are presented in Table 5. The predicted and measured resilient modulus values are in agreement.

Table 4
Summary of the laboratory cone test results

		Depth (m)	q_c (MPa)	f_s (MPa)	σ_c (kPa)	σ_v (kPa)	w (%)	γ_d (kN/m^3)
Silty clay	dry	0.31	1.5	0.0763	3.58	5.72	14.4	16.1
	opt.	0.31	1.8	0.0816	3.82	6.11	18.0	16.7
	wet	0.31	1.1	0.0705	3.80	6.08	21.8	16.1
Heavy clay	dry	0.31	1.3	0.0758	3.93	5.19	26.4	13.1
	opt.	0.31	1.6	0.1060	4.20	5.54	31.4	13.6
	wet	0.31	0.4	0.0965	4.09	5.40	36.4	12.8
Silt	dry	0.31	3.2	0.1622	3.03	5.72	10.7	16.4
	opt.	0.31	5.7	0.0032	3.28	6.17	15.2	17.2
	wet	0.31	0.9	0.0010	3.15	5.93	20.4	15.9
Sand	dry	0.31	2.9	0.0010	2.79	5.25	5.0	16.1
	opt.	0.31	7.6	0.0087	2.92	5.50	8.1	16.4
	wet	0.31	1.0	0.0300	2.86	5.39	11.0	15.7

Legend: M_r- resilient modulus, s_c- confining (minor principal) stress, s_v- vertical (major principal) stress, f_s- sleeve friction, w- water content, g_d- dry unit weight, g_w- unit weight of water, and q_c- cone resistance.

Table 5
Stress analysis for the laboratory cone tests

Soil type		Depth (m)	Controlled test-insitu			Controlled test-insitu & traffic		
			σ_c (kPa)	σ_d (kPa)	M_r (MPa)	σ_c (kPa)	σ_d (kPa)	M_r (MPa)
Silty clay	dry	0.31	3.58	2.14	46.20	7.88	11.30	39.36
	opt.	0.31	3.82	2.29	48.30	8.12	11.50	48.84
	wet	0.31	3.80	2.28	32.33	8.10	11.50	29.93
Heavy clay	dry	0.31	3.93	1.26	42.09	9.31	7.27	44.06
	opt.	0.31	4.20	1.34	43.20	9.62	7.37	42.67
	wet	0.31	4.09	1.31	26.63	9.43	7.43	25.08
Silt	dry	0.31	3.03	2.69	23.94	6.88	10.70	35.28
	opt.	0.31	3.28	2.89	35.18	7.15	10.90	40.21
	wet	0.31	3.15	2.78	13.85	7.04	10.80	18.00
Sand	dry	0.31	2.79	2.46	48.52	6.58	12.10	53.92
	opt.	0.31	2.92	2.58	52.35	6.63	12.10	57.84
	wet	0.31	2.86	2.53	17.27	6.49	12.00	23.31

Legend: σ_c - Confining stress , σ_d - Deviator stress, M_r - Resilient modulus

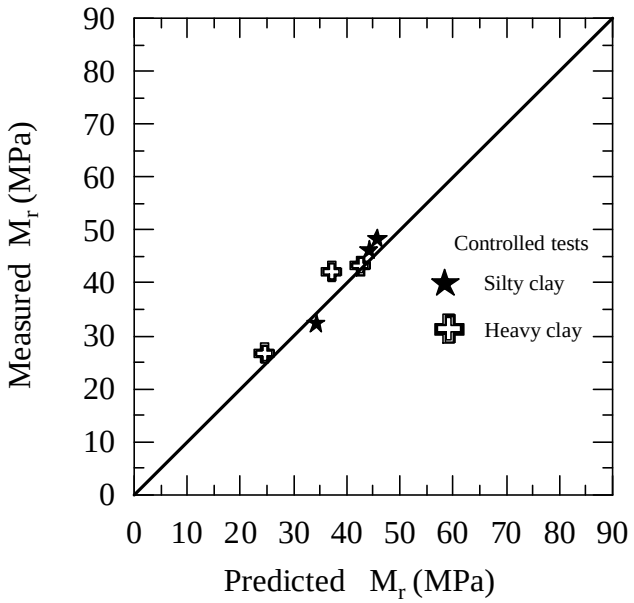

Figure 40
In-situ resilient modulus from the laboratory cone test for fine-grained soil

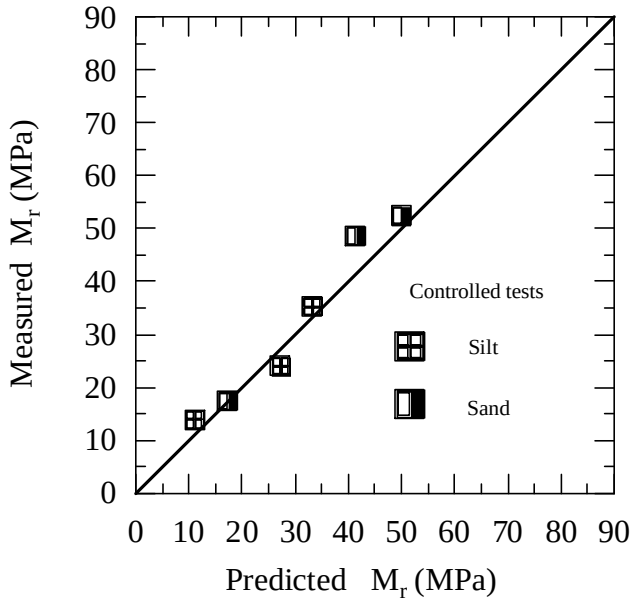

Figure 41
In-situ resilient modulus from the laboratory cone test for coarse-grained soil

Table 6
Elastic properties of the soil

Elastic Property	Silt	Sand
E (MPa)	27.1	45.9
n	0.35	0.35

Legend: E- Elastic modulus, *n*- Poisson's ratio

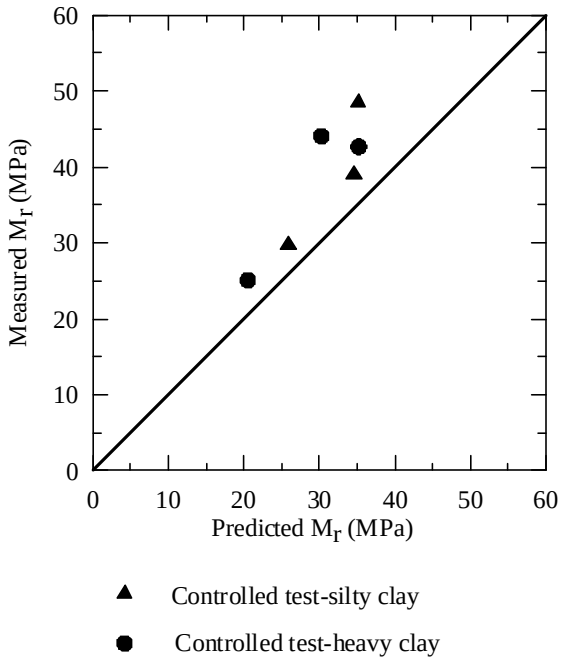

Figure 42
Prediction of resilient modulus from the traffic stress model for fine-grained soil

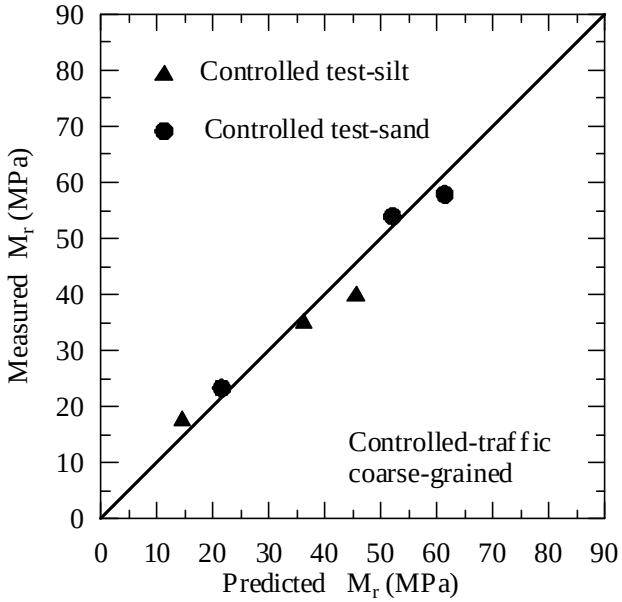

Figure 43
Prediction of resilient modulus from the traffic stress model for coarse-grained soil

Effect of Resilient Modulus on Overlay Thickness

The effect of change in the subgrade soil resilient modulus on the AASHTO flexible pavement design equation is analyzed. The AASHTO design equation *[1]*:

$$\log_{10} W_{18} = Z_R S_o + 9.36 \log_{10}(SN+1) - 0.20 + \frac{\log_{10}\left(\frac{\Delta PSI}{4.2-1.5}\right)}{0.40 + \frac{1094}{(SN+1)^{5.19}}} + 2.32 \log_{10} M_r - 8.07 \quad (8)$$

where,
W_{18}- predicted number of 18-kip equivalent single axle load (ESAL),
Z_R - standard deviation,
SN- structural number,
R- reliability,
S_o- combined standard error of the traffic prediction and performance prediction,
M_r- effective resilient modulus of subgrade soil, and
DPSI- difference between the initial design serviceability index and the design terminal serviceability index.

The AASHTO design equation is iteratively evaluated for a typical pavement section, by varying the value of the overlay thickness while keeping the design ESAL constant. The design variables are as follows. W_{18}= 5,000,000 ESALs, *R*= 95 %, S_o= 0.35, *DPSI*= 1.9, and design M_r= 34.5 MPa. This results in *SN* = 5. Layer coefficients are assumed as a_1= 0.01654/mm (0.42/in.), a_2= 0.0063/mm (0.16/in.) and a_3=0.0040/mm (0.10/in.) for the surface course, base, and subbase respectively. The thicknesses are D_1=102 mm, D_2=241 mm, and D_3=457 mm for the surface course, base, and subbase respectively.

Figure 44 shows the effect of the resilient modulus value on the thickness of the asphalt surface layer. Inspection of this figure demonstrates that reliable determination of the resilient modulus is important to avoid over-design or under-design of pavement layers. The change in the resilient modulus has a significant effect on the overlay thickness of a pavement.

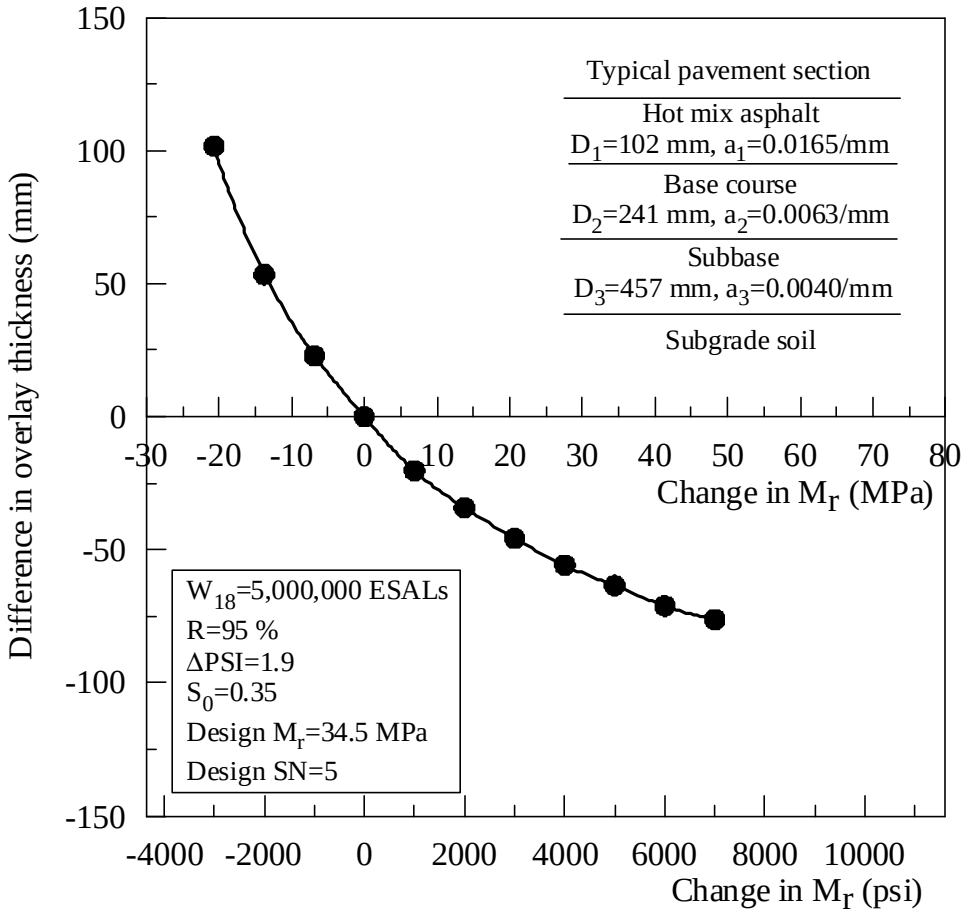

Figure 44

The effect of the resilient modulus of subgrade soils on the overlay design thickness

The Current Louisiana Department of Transportation and Development Procedure for Estimation of the Resilient Modulus

Currently, the LA DOTD procedure for estimating the resilient modulus of subgrade soils is based on the following correlation with the soil support value (SSV):

$$M_r = 1500 + 450\left(\left(\frac{53}{5}\right)(SSV - 2)\right) - 2.5\left(\left(\frac{53}{5}\right)(SSV - 2)\right)^2 \quad (9)$$

The soil support values used to determine the resilient modulus are obtained from a database, based on the parish system. In addition, the effective resilient modulus required by the AASHTO design guide should be determined based on the seasonal variations of the resilient modulus along the year. In the current method used by the LA DOTD, this cannot be achieved since one resilient modulus value is allocated for each parish. Figure 45 compares the resilient modulus values estimated from different methods. As shown in Figure 45, the resilient modulus values of the LA DOTD procedure are different from that of model, equation (1), predicted and laboratory measured. According to Figure 44, this difference makes a considerable change in the overlay thickness.

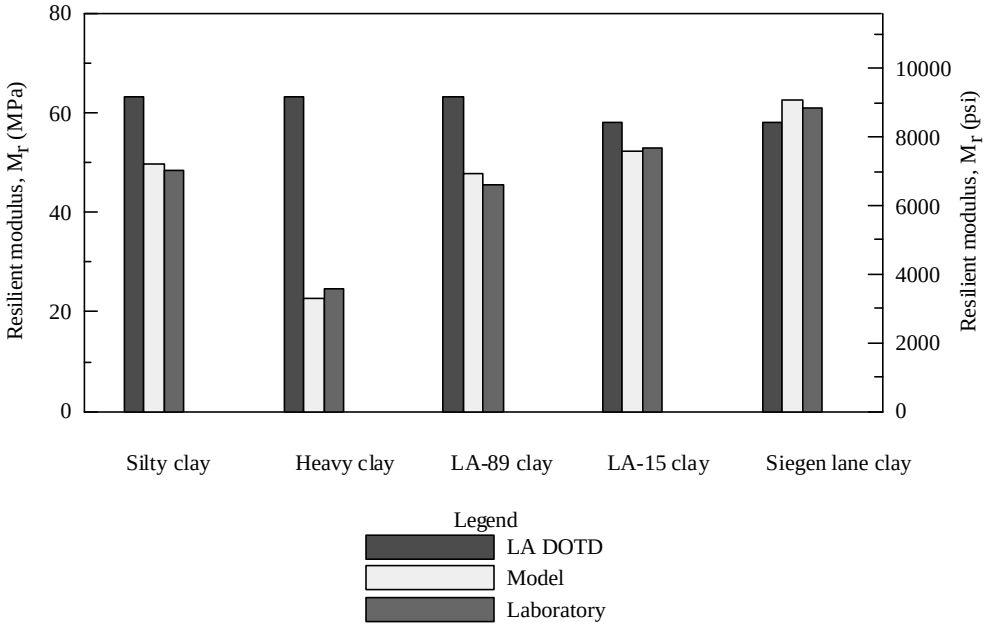

Figure 45
Comparison of the LA DOTD and model predicted resilient modulus

In the AASHTO pavement design method, the resilient modulus has a significant effect on the overlay thickness as shown in Figure 44. The method proposed in this report takes into account the soil type and properties on the resilient modulus of subgrade soils. That is why the results predicted by this method were in an agreement with the measured resilient modulus values.

Approximate Estimation of Unit Weight of Soils

The unit weight of soils may be estimated from a data base, subgrade soil survey, design records, results of nuclear density gauge test, or results of laboratory soil sample tests. Table 7 presents approximate dry unit weight values of typical soil types. Some of the dry unit weight values in Table 7 were obtained from the previous studies while the remaining was based on this study *[11]*, *[22]*. The unit weight can be estimated from Table 7.

As described in Figure 46, the cone penetration test parameters can be used to classify soils *[29]*, *[30]*. Table 7 along with the soil classification (Figure 46) can be used to estimate the unit weight of soils.

Comparison of Resilient Modulus Models

The cone tip resistance has a relationship to soil density *[30]*. Therefore, a model may be developed without dry unit weight parameter to predict the resilient modulus from cone penetration test parameters. For in-situ fine-grained soils, a statistical model was developed similar to the previous models by eliminating dry unit weight parameter in the analysis. This model is expressed as,

$$\frac{M_r}{s_c^{0.55}} = \frac{1}{s_v}\left(3.31 q_c\right) + \frac{2.9}{w} \qquad (10)$$

M_r- resilient modulus (Mpa),
s_c- confining (minor principal) stress (kPa),
s_v- vertical (major principal) stress (kPa),
q_c- tip resistance (MPa), and
w- water content (as a decimal).

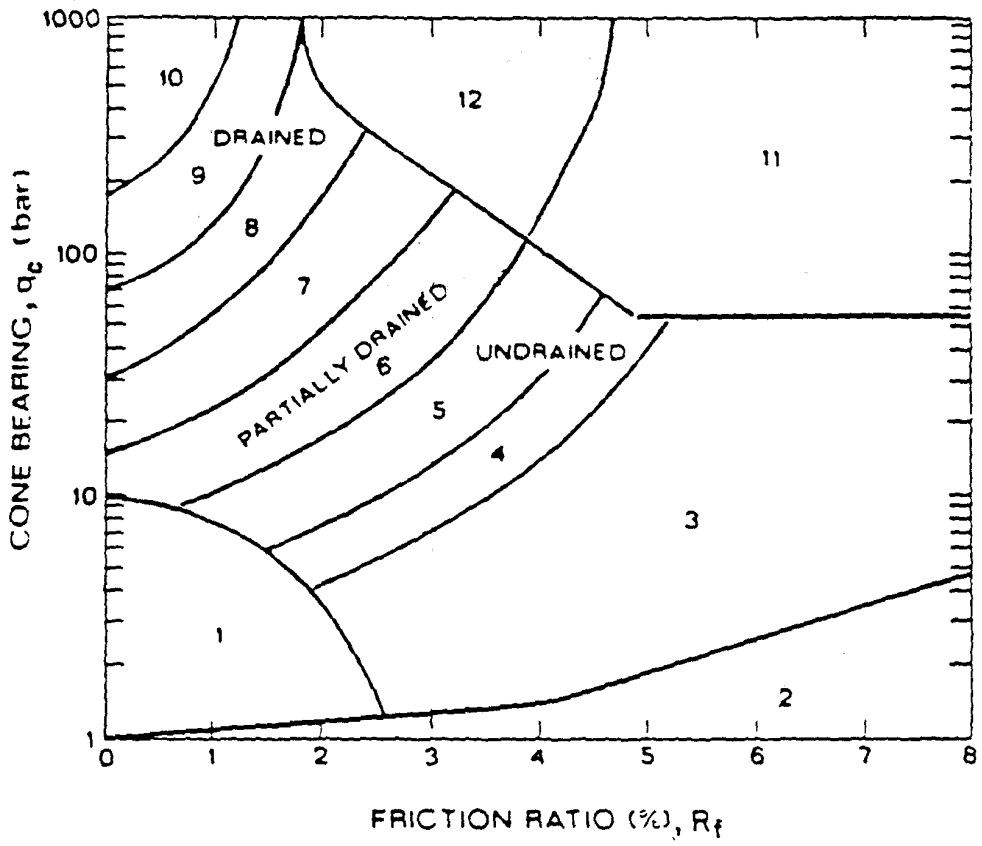

Zone: Soil Behavior Type

1. Sensitive fine grained	2. Organic material	3. Clay
4. Silty clay to clay	5. Clayey silt to silty clay	6. Sandy silt to clayey silt
7. Silty sand to sandy silt	8. Sand to silty sand	9. Sand
10. Gravelly sand to sand	11. Very stiff fine grained*	12. Sand to clayey sand*

* Overconsolidated or cemented

Note: 1 bar = 100 kPa = 14.5 psi

Figure 46
A soil classification chart for friction cone *[30]*

Table 7
Typical values of dry unit weight of soils

Soil type	Approximate dry unit weight, γ_d (kN/m^3)
Silty clay	16.7
Heavy clay (Fat clay)	13.6
Clay* (30%-50% clay sizes)	17.8
Colloidal clay* (-0.002 mm: 50%)	16.8
Fine sand (poorly graded sand)	16.4
Standard Ottawa sand*	17.5
Clean , uniform sand* (fine or medium)	18.7
Silt (silty sand, sandy loam)	17.2
Uniform inorganic silt*	18.7
Silty sand* (well graded)	20.2
Clean, fine to coarse sand* (well graded)	21.9
Silty sand and gravel* (well graded)	23.2
Sandy or silty clay*	21.4
Well graded gravel, sand, silt & clay mixture*	23.5
Organic silt*	17.5
Organic clay* (30%-50% clay sizes)	15.9
Sensitive fine grained**	17.5
Organic material**	12.5
Clayey silt to silty clay**	18.0
Sandy silt to clayey silt**	18.0
Silty sand to sandy silt**	18.5
Sand to silty sand**	19.0
Sand**	19.5
Gravelly sand to sand**	20.0
Very stiff fine-grained (overconsolidated or cemented)**	20.5
Sand to clayey sand (overconsolidated or cemented)**	19.0

Legend: *- *[22]* and **- *[11]*

For this correlation, the coefficient of determination, $R^2 = 0.98$ and root mean squared error, RMSE = 1.55.

The resilient modulus values of soils were estimated by using the model given in equation (1) (referred to as Mohammad model), the model given in equation (10) (referred to as without dry unit weight model), and the model given in equation (1) with dry unit weight estimated from Table 7 (referred to as M_r from dry unit weight table). These resilient modulus values of soils were compared with the resilient modulus values obtained from laboratory testing (referred to as M_r from laboratory). Figure 47 shows the comparison among these resilient modulus values. The difference between the resilient modulus values of Mohammad model and laboratory measured is small. According to Figure 44, this small difference makes no considerable change in the overlay thickness.

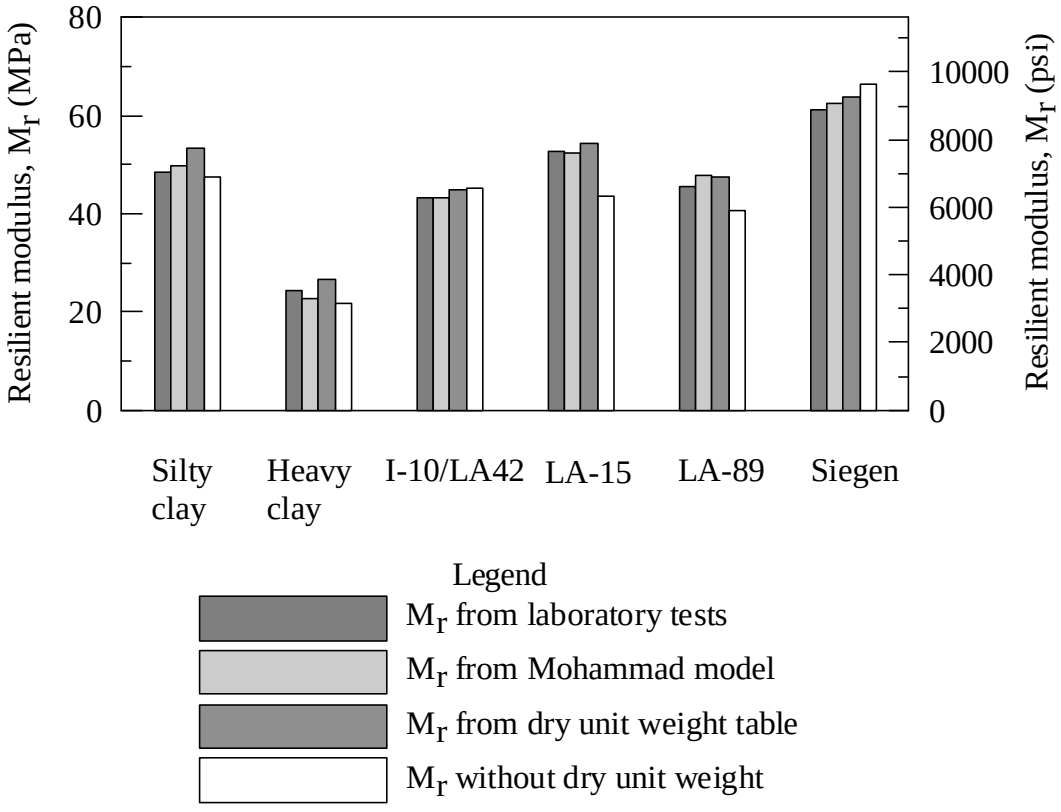

Figure 47
Comparison of different methods for estimating resilient modulus

The maximum difference between the resilient modulus values estimated, based on the dry unit weight table, and laboratory measured is 4.9 MPa or percent error is 10 %. According to Figure 44, this difference makes a small change in the overlay thickness. The maximum difference between the resilient modulus values estimated, based on the without dry unit weight model, and laboratory measured is 9.1 MPa or percent error is 17 %. According to Figure 44, this difference makes a considerable change in the overlay thickness. Therefore, the model without dry unit weight is not recommended.

The Use of Models in Predicting the Seasonal Variations in Resilient Modulus

The AASHTO guide for design of pavement structures stipulates that the subgrade soils be analyzed for different moisture seasons in a year, such as dry and rainy, to estimate an effective resilient modulus for the design purpose *[1]*. Covering the primary moisture seasons, such as dry and rainy, the resilient modulus tests (AASHTO T 294) should be performed on roadbed soil samples. By knowing the seasonal resilient moduli of roadbed soil, the relative damage (U_r) of the pavement can be estimated. From the relative damage, an effective resilient modulus value for flexible pavements can be obtained by using the design charts and equations provided by the AASHTO guide for design of pavement structures. The same design charts can be used while being modified the estimation of the resilient modulus from the cone penetration test results. This procedure consists of performing several cone penetration tests in different moisture seasons in a year, estimating corresponding moisture content, unit weight of soil, and soil stresses. The moisture content and unit weight may be estimated by using a nuclear gauge, from a subgrade soil survey or testing on soil samples. Seasonal resilient modulus for each month can be evaluated by using the correlation proposed in this study. The relative damage can be estimated by the equation (11), given in the AASHTO guide for design of pavement structures *[1]*. The effective design resilient modulus can be estimated from the average relative damage and the AASHTO equation (12). The effective resilient modulus, corresponding to the average relative damage, can be estimated.

Steps in this procedure:

1. As shown Figure 48, divide a year into one-month or one-half month seasons. All the seasons (time periods in the chart) in a year must be equal.
2. Allocate the seasonal tip resistance, sleeve friction, moisture content, dry unit weight, confining stress, and deviator stress in their respective time slots.
3. Compute the seasonal resilient modulus by using the proposed correlations.

4. Estimate the relative damage by using the charts or equations given in the AASHTO guide for design of pavement structures *[1]*.
5. Add the all relative damage values and compute an average relative damage value.
6. Estimate an effective resilient modulus, corresponding to the average relative damage, by using the charts or equations given in the AASHTO guide for design of pavement structures *[1]*.

In the case of rigid pavements, an effective modulus of subgrade reaction (k-value) must be calculated from the seasonal roadbed soil resilient modulus with the aid of the charts or equations given in the AASHTO guide for design of pavement structures.
Average relative damage,

$$U_r = \frac{\sum U_r}{n} \tag{11}$$

The AASHTO *[1]* equation for relative damage,

$$U_r = 1.18 x 10^8 x M_r^{-2.32} \tag{12}$$

Month	q_c (MPa)	f_s (MPa)	w (%)	γ_d (kN/m^3)	σ_c (kPa)	σ_d (kPa)	M_r (psi)	U_r
Jan.								
Feb.								
March								
April								
May								
June								
July								
August								
Sept.								
Oct.								
Nov.								
Dec.								
Total								ΣU_r

Legend: U_r -relative damage, n - number of months, M_r- resilient modulus (*psi*)

Figure 48
A chart for estimating effective roadbed soil resilient modulus using the serviceability criteria

The Use of the Models in Predicting the Resilient Modulus Profile

Since the cone penetration test results provides a continuous profile of the soil, the proposed models can be used to predict the resilient modulus profile of the soil along the depth. This method provides a continuous measurement of the soil stiffness along the depth. This has several practical applications in pavement designs, rehabilitations, and quality control and quality assurance (QC/QA). Figure 49 shows the resilient modulus profile of silty clay dry side.

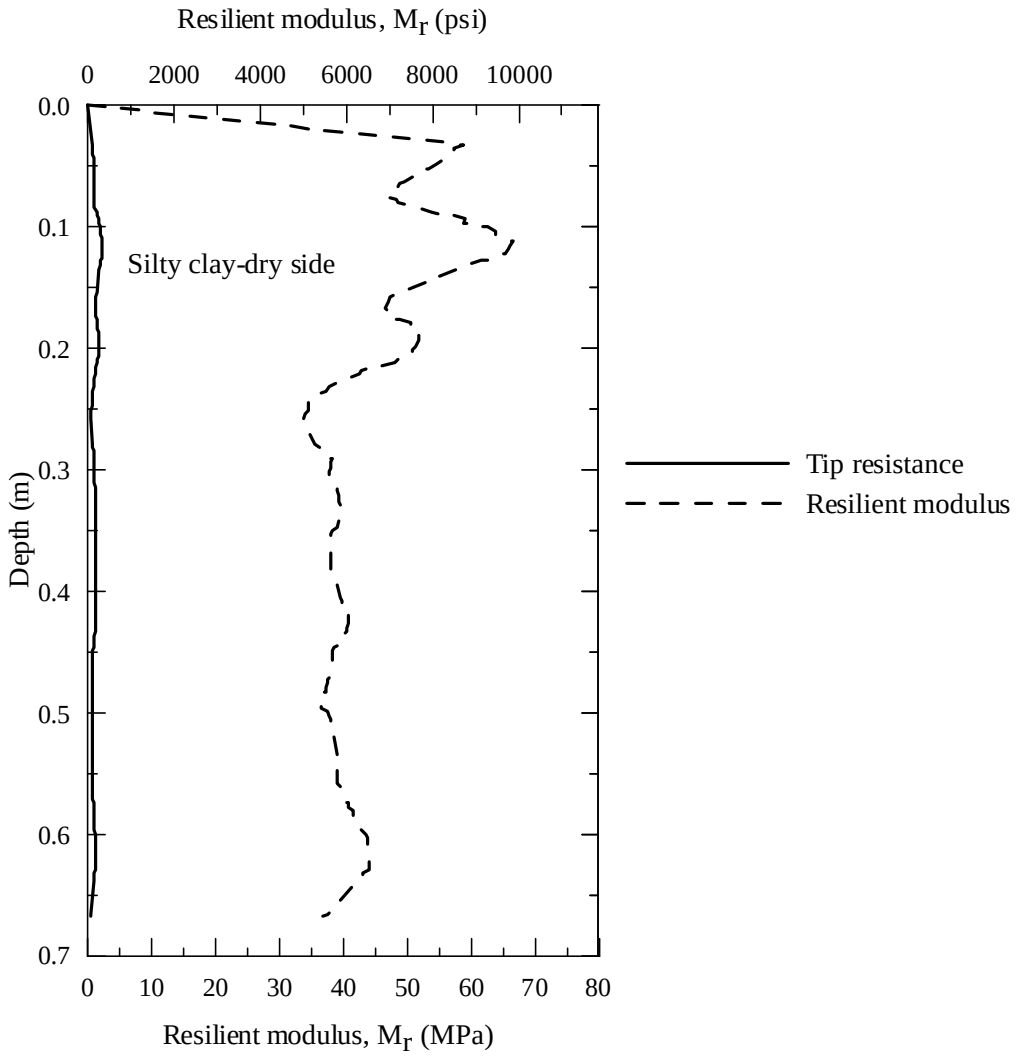

Figure 49
The resilient modulus profile of silty clay dry side

SUMMARY AND CONCLUSIONS

This report presents findings of a study to evaluate the effect of the moisture content and soil dry unit weight on the resilient modulus predicted using the intrusion technology. Laboratory cone penetration tests, repeated load triaxial test, and soil property tests were performed on laboratory compacted soil samples to investigate the effects of the variation in the moisture content and unit weight on the resilient modulus as well as to validate the models, developed during phase I of this research.

Major findings of this investigation are summarized below:

(1) The resilient modulus prediction models, developed in phase I of this study, were validated with the laboratory cone test results. The predicted and measured resilient modulus values from these models were in agreement.

(2) The resilient modulus increases with the moisture content up to the optimum and then it decreases. There is a combined effect from the moisture content and unit weight on the resilient modulus of soil. The maximum resilient modulus and tip resistance occurred at the optimum.

(3) A sensitivity analysis was performed to evaluate the effect of the change in the resilient modulus, due to variations in dry unit weight and moisture content, on the overlay thickness.

(4) The change in the subgrade resilient modulus results in a significant change in the pavement overlay thickness.

(5) The proposed models can be used to predict the seasonal variations of the resilient modulus.

(6) The unit weight may be estimated from a data base, subgrade soil survey, design records, test results of a nuclear density gauge, or testing on soil samples.

RECOMMENDATIONS

The proposed procedure is to be implemented in pavement designs, rehabilitation, and quality control and quality assurance. A software program is to be developed to implement the proposed models in these pavement applications.

LIST OF ABBREVIATIONS

AASHTO	American Association of State Highway and Transportation Officials
ALF	Accelerated Load Facility
ASTM	American Society for Testing and Materials
BH	Borehole
c	Cohesion intercept
CBR	California Bearing Ratio
CICU	Isotropically Consolidated Undrained Triaxial Compression Test
COV	Coefficient of Variation
CPT	Cone Penetration Test
CIMCPT	Continuous Intrusion Miniature Cone Penetrometer Test
E	Modulus of Elasticity (Young's modulus)
ESAL	Equivalent Single Axial Loading
EMCRF	Engineering Materials Characterization Research Facility
FWD	Falling Weight Deflectometer
f_s	Sleeve friction
G_s	Specific gravity
k_o	Coefficient of lateral earth pressure at rest
LA DOTD	Louisiana Department of Transportation and Development
LCD	Liquid Crystal Display
LL	Liquid Limit
LTRC	Louisiana Transportation Research Center
LVDT	Linear Variable Differential Transducer
MTS	Material Testing System
M_r	Resilient modulus
MCPT	Miniature Cone Penetrometer Test
NA	Not available
NDT	Nondestructive Test
PCPT	Piezocone penetration test
PI	Plasticity Index
PL	Plasticity Limit
PRF	Pavement Research Facility
q_c	Cone tip resistance
R	Reliability
R^2	Coefficient of determination

REVEGITS	Research Vehicle for Geotechnical In-situ Testing and Support
RMSE	Root Mean Squared Error
R_f	Friction ratio
SAS	Statistical Analysis System
SHRP	Strategic Highway Research Program
SN	Structural number
S_o	Combined standard error of the traffic prediction and performance prediction
SSV	Soil Support Value
STD	Standard deviation
S_u	Undrained shear strength
TRB	Transportation Research Board
USCS	Unified Soil Classification System
UU	Unconsolidated Undrained Triaxial Compression Test
U_r	Relative damage
w	water content
w_{opt}	Optimum water content
W_{18}	Predicted number of 18-kip equivalent single axle load
Z_R	Standard normal deviation
γ_d	Dry unit weight
γ_{dmax}	Maximum dry unit weight
γ_w	Unit weight of water
ε_r	Axial strain
υ	Poisson's ratio
σ_1	Major principal stress
σ_3	Minor principal stress
σ_c	Confining stress
σ_d	Deviator stress
σ_h	Horizontal stress
σ_v	Vertical stress
f	Angle of internal friction
ΔPSI	Difference between the initial design serviceability index and the design terminal serviceability index.

REFERENCES

1. AASHTO Guide for Design of Pavement Structures, American Association of State Highway and Transportation Officials, 1993 and 2002.

2. AASHTO T 294-94, American Association of State Highway and Transportation Officials, "Resilient Modulus of Unbound Granular Base/Subbase Materials and Subgrade Soils-SHRP Protocol P46." AASHTO, T 294-94, 1995, pp. 794–807.

3. Allen, A.J. "Development of a correlation between physical and fundamental properties (resilient modulus) of Louisiana soils." Master's Thesis, Dept. of Civil Engineering, Louisiana State University, Baton Rouge, 1996.

4. Allen, D.L. "M_r Testing in Kentucky." Workshop on Resilient Modulus Testing, Oregon State University, Corvallis, 1989.

5. Carmichael III, R.F.and Stuart, E. "Predicting Resilient Modulus: A study to determine the mechanical properties of subgrade soils." TRB, No. 1043, 1986.

6. Drumm, E.C.; Reeves, J.S.; Madgett, M.R.; and Trolinger, W.D. "Subgrade Resilient Modulus Correction for Saturation Effects." *Journal of Geotechnical and Geoenvironmental Engineering*, Vol. 123, No.7, July 1997, pp. 663–670.

7. Fredlund, D.G.; Bergan, A.T.; and Wong, P.K.; "Relation Between Resilient Modulus and Stress Conditions for Cohesive Subgrade Soils." *Transportation Research Record*, No. 642, 1977, pp.73–81.

8. Holden, J.C. "Laboratory Research on Static Cone Penetrometers." Internal Report CE-SM-71-1, Dept. of Civil Engineering, University of Florida, Gainesville, Florida, U.S.A., 1971.

9. Kamal, M. A.; Dawson, A.R.; Farouki, O.T.; Hughes, D.A.B.; and Sha'at, A.A. "Field and Laboratory Evaluation of the Mechanical Behavior of Unbound Granular Materials in Pavements." *Transportation Research Record*, No. 1406, 1993, pp. 88–97.

10. Lee, K.W.; Marcus, A.S.; and Mao, H. "Determination of Effective Soil Resilient Modulus and Estimation of Layer Coefficients for Unbound Layers of Flexible Pavement in Rhode Island." Report No. URI-CVET-94-1 Res Rept No. 1, 1994.

11. Lunne, T.; Robertson, P.K.; and Powell, J.J.M. *Cone Penetration Testing in Geotechnical Practice*. Blackie Academic and Professional, London, 1997.

12. Mohammad, L.N.; Huang, B.; Puppala, A.; and Alen, A. "A Regression Model for Resilient Modulus of Subgrade Soils," *78th Annual Meeting of the Transportation Research Board*, Washington D.C., 1999.

13. Mohammad, L.N.; Alavilli, P.; and Puppala, A.J. "Data Acquisition System for Determining the Resilient Modulus of Soils." *ASCE Geotechnical special publication 37*, Advances in Site Characterization: Data Acquisition, Management and Interpretation, Dallas, 1993, pp. 27–41.

14. Mohammad, L. N.; Puppala, A. J.; and Alavilli, P. "Influence of Testing Procedure and LVDT Location on Resilient Modulus of Soils." *Transportation Research Record, No. 1462,* 1994, pp. 91–101.

15. Mohammad, L. N.; Puppala, A.; and Alavilli, P. "Effect of Strain Measurements on Resilient Modulus of Granular Soils." *Dynamic Geotechnical Testing*, Second Volume, ASTM STP 1213, ASTM, 1994, pp. 202–221.

16. Mohammad, L. N.; and Puppala, A. "Resilient Properties of Laboratory Compacted Subgrade Soils." National Academy of Science, *Transportation Research Record*, No. 1504, 1995, pp. 87–102.

17. Mohammad, L.N.; Titi, H.H.; and Herath, A. "Evaluation of Resilient Modulus of Subgrade Soil by Cone Penetration Test Results." Seventh International Conference on Low-Volume Roads, *Transportation Research Records*, No. 1652, Vol. 1, Baton Rouge, Louisiana, May 1999, pp. 236–245.

18. Mohammad, L.N.; Titi, H.H.; and Herath A. “Intrusion Technology: An Innovative Approach to Evaluate Resilient Modulus of Subgrade Soil.” Application of Geotechnical Principles in Pavement Engineering, *American Society of Civil Engineers*, Geotechnical Special Publication Number 85, Geo Congress’98, Boston, Massachusetts, Oct.1998, pp. 39–58.

19. Mohammad, L.N.; Titi, H.H.; and Herath A. “Investigation of the Applicability of Intrusion Technology to Estimate the Resilient Modulus of Subgrade Soil.” Final Report, Louisiana Transportation Research Center project No. 98-6GT, April 2000.

20. Monismith, C.L. “M_r testing- Interpretation of Laboratory Results for Design Purposes.” Workshop on Resilient Modulus Testing, Oregon State University, Corvallis, 1989.

21. Nataatmadja, A.; and Parkin, A. “Characterization of Granular Materials for Pavements.” *Canadian Geotechnical Journal*, Vol.26, No.4, 1989, pp. 725–730.

22. Naval Facilities Engineering Command. *Soil Mechanics Design Manual 7.01 (DM-7)*, 200 Stovall Street, Alexandria, Virginia, 1986, p. 7.1-22.

23. Nazarian, S.; and Feliberti, M. “Methodology for Resilient Modulus Testing of Cohesionless Subgrades.” *Transportation Research Record*, No. 1406, 1993, pp. 108–115.

24. Parkin, A.K.; and Lune, T. “Boundary Effects in the Laboratory Calibration of a Cone Penetrometer for Sand.” *Proceedings of the European Symposium on Penetration Testing*, Vol.2, Amsterdam, 1982, pp. 761–768.

25. Pezo, R.; and Hudson, W.R. “ Prediction Models of Resilient Modulus for Nongranular Materials.” *Geotechnical Testing Journal*, Vol.17, No.3, 1994, pp. 349–355.

26. Puppala, A.; Mohammad, L.N.; and Allen, A. “Rutting Potential of Subgrade Soils from Repeated Load Triaxial Resilient Modulus Test.” *ASCE Journal of Materials in Civil Engineering*, Vol. 11, No. 4, Nov. 1999, pp. 274–282.

27. Rada, G.; and Witczak, M.W. " Comprehensive Evaluation of Laboratory Resilient Moduli Results for Granular Material." *Transportation Research Record*, No. 810, 1981, pp. 23–33.

28. Robertson, P.K.; and Campanella, R.G. "Interpretation of Cone Penetration Tests- Part II: Clay." *Canadian Geotechnical Journal*, Vol.20, No.4, 1983, pp. 734–745.

29. Robertson, P.K.; and Campanella, R.G. *Guidelines for Use and Interpretation of the Electric Cone Penetration Test*, Hogentogler & Company, Inc., Gaithersburg, MD, Second Edition, 1984, p. 175.

30. Robertson, P.K.; and Campanella, R.G. *Guidelines for Geotechnical Design Using CPT and CPTU*, Soil Mechanics Series No. 120, Department of Civil Engineering , University of British Columbia, Vancouver, B.C., V6T 1W5, Canada, 1989.

31. Schmertmann, J.H. *Guidelines for Cone Penetration Test: Performance and Design*, Report No. FHWA-TS-78-209. Federal Highway Administration, Washington, D.C., 1978, pp. 145.

32. Sebaaly, P.E.; Tabatabaee, N.; and Scullion, T. "Comparison of Backcalculated Moduli from Falling Weight Deflectometer and Truck Loading." *Transportation Research Record*, No. 1377, 1992, pp. 88–98.

33. Tumay, M.T.; Kurup, P.U.; and Boggess, R.L. "A continuous intrusion electronic miniature cone penetration test system for site characterization." Geotechnical Site Characterization, *Proc. 1st International Conf. On site characterization-ISC'98*, Vol. 1, Atlanta, 1998, pp. 1183–1188.

34. Tumay, M.T.; and Kurup, P.U. "Calibration and Implementation of Miniature Electric Cone Penetrometers for Road and Highway Design and Construction Control." LTRC State Project No. 736-13-0036, 1997.

35. Ullidtz, P. *Pavement Analysis*, Elsevier Publications, New York, 1987.

36. Uzan, J. "Characterization of Granular Materials." *Transportation Research Record*, No. 1022, TRB, 1985, pp. 52–59.

37. Wissa, A.E.; Martin, R.T.; and Garlanger, J.E. “The Piezometer Probe.” Proc., ASCE Conference on In-Situ Measurement of Soil Properties, Vol. 1, Raleigh, NC, 1975, pp. 536-545.

APPENDIX A

Table A1
Resilient modulus test results for silty clay at the controlled test

σ_c (kPa)	σ_d (kPa)	M_r (MPa) dry side	COV (%)	M_r (Mpa) optimum	COV (%)	M_r (MPa) wet side	COV (%)
41	14	59.57	4.1	79.09	2.0	38.01	3.4
41	28	55.84	5.5	74.10	1.9	37.69	4.6
41	41	51.54	5.2	69.07	1.7	36.91	4.6
41	55	47.87	2.1	64.92	4.8	36.47	7.6
41	69	45.96	7.5	62.18	2.7	35.28	8.3
21	14	46.70	5.2	63.18	5.5	32.69	2.4
21	28	41.28	7.4	57.82	2.1	31.89	3.6
21	41	38.81	7.3	54.28	4.3	31.21	6.1
21	55	37.72	3.2	51.18	5.4	30.56	7.7
21	69	36.99	5.6	49.99	3.9	29.37	6.7
0	14	34.66	7.6	40.27	4.2	27.43	9.9
0	28	30.67	9.3	39.44	2.3	26.44	9.4
0	41	29.08	9.2	38.77	3.5	25.65	8.1
0	55	28.57	9.3	38.42	5.5	24.86	9.7
0	69	28.06	7.6	38.23	8.7	24.43	9.2

Table A2
Resilient modulus test results for heavy clay at the controlled test

σ_c (kPa)	σ_d (kPa)	M_r (MPa) dry side	COV (%)	M_r (MPa) optimum	COV (%)	M_r (MPa) wet side	COV (%)
41	7	61.29	2.8	60.69	2.4	40.38	4.3
41	14	59.11	1.8	56.55	3.8	38.60	3.2
41	21	57.11	2.1	54.34	1.5	38.43	4.9
21	7	54.27	2.7	51.92	4.0	29.51	5.8
21	14	52.03	2.0	49.42	6.1	28.51	6.3
21	21	50.11	2.1	47.69	2.7	26.85	8.5
0	7	37.43	5.8	36.34	5.0	21.94	9.4
0	14	36.90	5.4	34.78	2.9	20.76	8.0
0	21	36.57	3.3	34.05	3.8	20.04	9.8

Table A3
Resilient modulus test results for silt at the controlled test

σ_c (kPa)	σ_d (kPa)	M_r (MPa) dry side	COV (%)	M_r (MPa) optimum	COV (%)	M_r (MPa) wet side	COV (%)
21	21	58.94	4.1	56.25	5.3	33.94	9.5
21	41	60.51	3.2	56.82	5.6	34.80	7.2
21	62	64.27	4.6	57.39	9.0	35.42	4.7
34	34	78.03	2.9	76.98	4.3	60.82	4.2
34	69	80.81	3.0	77.62	3.6	61.92	4.2
34	103	82.37	4.6	78.39	4.6	63.27	5.0
69	69	121.33	3.3	110.21	2.8	103.52	2.5
69	138	126.62	4.3	111.23	3.6	104.70	2.8
69	207	126.45	3.0	113.71	3.2	105.12	3.1
103	69	155.98	3.1	135.29	2.4	146.27	1.7
103	103	157.93	2.0	136.35	2.5	148.48	2.3
103	207	164.00	1.6	137.40	3.4	151.41	1.7
138	103	187.01	1.5	165.13	2.0	180.67	1.7
138	138	189.94	1.8	167.21	1.7	182.84	2.3
138	276	191.98	1.8	167.90	2.8	184.16	1.9

Table A4
Resilient modulus test results for sand at the controlled test

σ_c (kPa)	σ_d (kPa)	M_r (MPa) dry side	COV (%)	M_r (MPa) optimum	COV (%)	M_r (MPa) wet side	COV (%)
21	21	75.51	2.2	79.17	3.1	42.92	7.6
21	41	75.97	2.1	79.79	4.2	43.74	3.0
21	62	76.71	2.3	80.49	3.8	45.04	3.3
34	34	105.00	2.0	107.68	3.0	70.20	3.7
34	69	106.00	2.1	108.39	3.2	70.75	5.5
34	103	107.15	1.9	110.00	2.3	72.06	4.6
69	69	172.58	1.3	174.07	1.4	143.99	2.7
69	138	171.05	1.4	174.76	1.8	144.17	2.7
69	207	165.74	1.5	171.34	1.3	146.58	1.5
103	69	220.66	1.0	234.07	1.9	213.99	1.6
103	103	225.22	0.9	237.06	1.1	217.50	1.6
103	207	220.71	0.8	234.30	1.3	214.19	1.5
138	103	257.80	0.9	271.46	1.4	251.97	1.8
138	138	262.22	0.8	276.17	1.5	255.39	1.2
138	276	252.64	1.1	271.56	0.9	246.28	1.0